KfK 5073
September 1992

Theory of Neutron Resonance Cross Sections for Safety Applications

F. H. Fröhner
Institut für Neutronenphysik und Reaktortechnik
Projekt Nukleare Sicherheitsforschung

Kernforschungszentrum Karlsruhe

KERNFORSCHUNGSZENTRUM KARLSRUHE
Institut für Neutronenphysik und Reaktortechnik
Projekt Nukleare Sicherheitsforschung

KfK 5073

THEORY OF NEUTRON RESONANCE CROSS SECTIONS FOR SAFETY APPLICATIONS

F.H. Fröhner

Kernforschungszentrum Karlsruhe GmbH, Karlsruhe

Als Manuskript gedruckt
Für diesen Bericht behalten wir uns alle Rechte vor

Kernforschungszentrum Karlsruhe GmbH
Postfach 3640, 7500 Karlsruhe 1

ISSN 0303-4003

THEORIE DER NEUTRONEN-RESONANZQUERSCHNITTE FÜR SICHERHEITSANWENDUNGEN

ZUSAMMENFASSUNG

Neutronenresonanzen bestimmen ganz wesentlich das Betriebsverhalten von Kernreaktoren, besonders das Reagieren auf den Temperaturanstieg bei Leistungsexkursionen, und ebenso die Wirksamkeit von Abschirmmaterialien. Die benötigte Theorie der Wirkungsquerschnitte für neutroneninduzierte Resonanzreaktionen wird vorgestellt, einschließlich der praktisch wichtigen Näherungen sowohl für den Bereich aufgelöster wie auch für den Bereich nicht aufgelöster Resonanzen. Numerische Verfahren zur Berechnung der Doppler-Verbreiterung von Resonanzen werden diskutiert, und die Erzeugung von Gruppenkonstanten und speziell von Selbstabschirmfaktoren für Neutronikrechnungen wird umrissen.

THEORY OF NEUTRON RESONANCE CROSS SECTIONS FOR SAFETY APPLICATIONS

ABSTRACT

Neutron resonances exert a strong influence on the behaviour of nuclear reactors, especially on their response to the temperature changes accompanying power excursions, and also on the efficiency of shielding materials. The relevant theory of neutron resonance cross sections including the practically important approximations is reviewed, both for the resolved and the unresolved resonance region. Numerical techniques for Doppler broadening of resonances are presented, and the construction of group constants and especially of self-shielding factors for neutronics calculations is outlined.

This review paper was prepared for the "Workshop on Computation and Analysis of Nuclear Data Relevant to Nuclear Energy and Safety", held at the International Centre for Theoretical Physics, Trieste, Italy, 10 February - 13 March 1992.

CONTENTS

THEORY OF NEUTRON RESONANCE CROSS SECTIONS FOR SAFETY APPLICATIONS

F.H. Fröhner
Kernforschungszentrum Karlsruhe
Institut für Neutronenphysik und Reaktortechnik
Postfach 3640, W-7500 Karlsruhe 1
Germany

ABSTRACT. Neutron resonances exert a strong influence on the behaviour of nuclear reactors, especially on their response to the temperature changes accompanying power excursions, and also on the efficiency of shielding materials. The relevant theory of neutron resonance cross sections including the practically important approximations is reviewed, both for the resolved and the unresolved resonance region. Numerical techniques for Doppler broadening of resonances are presented, and the construction of group constants and especially of self-shielding factors for neutronics calculations is outlined.

1. Introduction: Neutron Resonances and Neutron Flux

If nuclei of a given species, e. g. ^{235}U, are bombarded by neutrons, one observes nuclear reactions such as elastic scattering, radiative capture, or fission. The probabilities for those (n,n), (n,γ), or (n,f) processes, customarily expressed as cross sections in units of barn (1 b = 10^{-24} cm^2), depend sensitively on the energies of the incident neutrons. The scattering cross section, for instance, is mostly close to the geometrical cross section of the nuclei (several barns) but at certain energies it rises suddenly by several orders of magnitude. Similar resonance behaviour, at the same energies, is exhibited by the capture and fission cross sections. Fig. 1 (top and middle) show this behaviour for the nucleus ^{238}U for which elastic scattering and radiative capture are the only energetically allowed neutron reactions at low energies. For ^{235}U one would see resonances also in fission in this energy range. Each of these resonances is due to excitation of a relatively long-lived (quasi-stationary) state of the compound nucleus that is formed temporarily if a neutron interacts with a target nucleus. Note the different resonance shapes: Those of the capture cross section are symmetric whereas those of the scattering cross section are asymmetric, with pronounced minima and sizable "potential" scattering between resonances.

The impact of the resonances on the neutron spectrum in a power reactor is shown in Fig. 1 (bottom). The conspicuous dips in the neutron flux coincide with the resonance peaks in the cross sections. The explanation is simple: Neutrons cannot survive long at energies where ^{238}U, the main fuel constituent, has high cross sections, because there they are soon captured (removed completely) or scattered (transferred to some other, usually

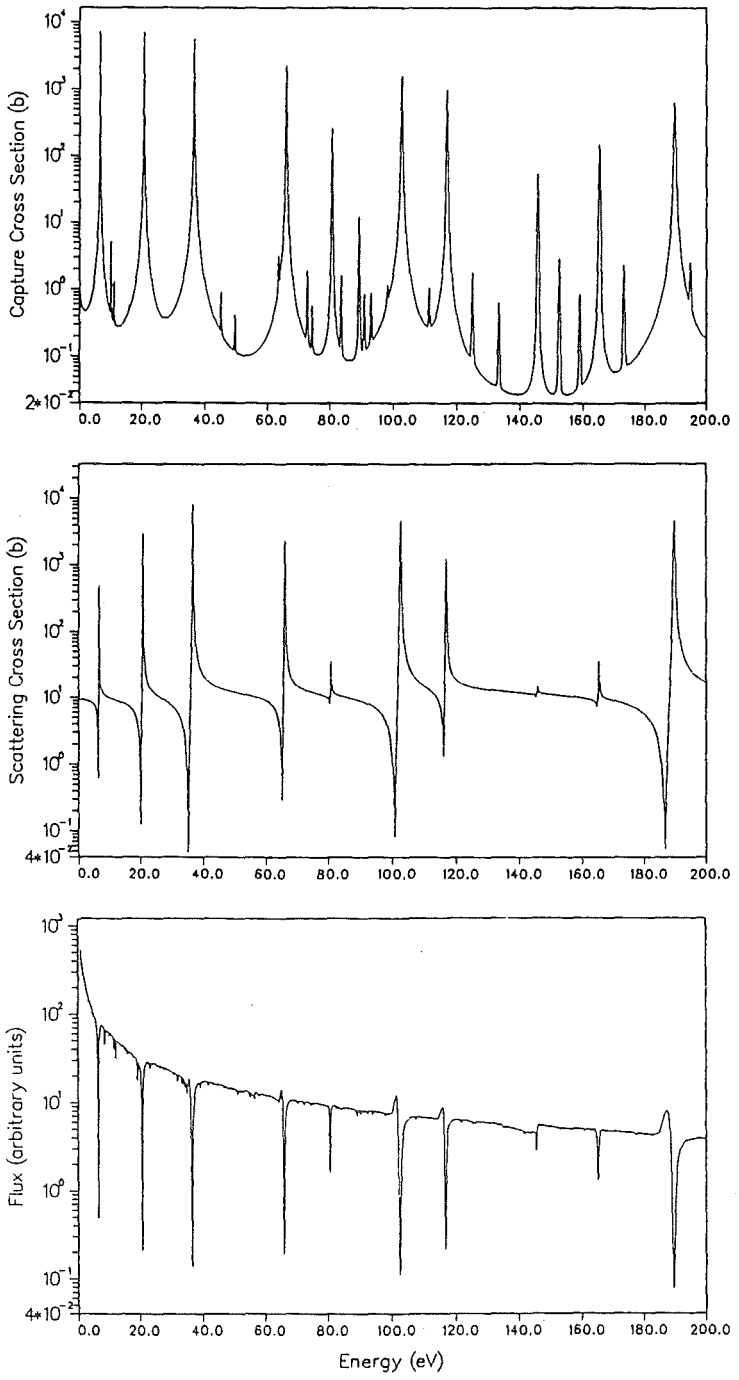

Fig. 1. Top: ^{238}U neutron capture cross section below 200 eV, Doppler broadened to 300 K. Middle: ^{238}U neutron scattering cross section, broadened to 300 K. Bottom: Neutron spectrum in an advanced pressurised-water reactor (C. Broeders, KfK, private communication). Note the logarithmic ordinate scales. Energies are given in the laboratory system.

lower) energy. As a result the flux is depleted at the ^{238}U resonances. Smaller dips in the flux are due to other, less abundant fuel components such as the fissile ^{235}U.

At low energies the resonances appear fairly well separated but as the energy increases their spacings decrease while their widths increase. Eventually they overlap so much that the compound resonance structure is averaged out and only the much broader structures survive, such as the size (or single-particle) resonances described by the optical model or the giant dipole resonances observed in photonuclear reactions. As a rule only the resonances at relatively low energies can be observed directly. At intermediate energies they are not fully resolved because of limited instrumental resolution, although the real disappearance of compound resonance structure due to excessive level overlap occurs only at still higher energies. Thus one distinguishes the resolved resonance region from the unresolved (or at best partially resolved) resonance region.

The more nucleons belong to the compound system the finer is the resonance structure. Typical level spacings observed in neutron reactions are of the order

MeV	for light,
keV	for medium-weight,
eV	for heavy nuclei.

The level spacings of even target nuclei (nucleon number even) are generally larger than those of odd ones (nucleon number odd). Magic or near-magic nuclei have untypically large level spacings. The heavy, doubly-magic nucleus ^{208}Pb, for instance, has level spacings resembling those of light nuclei.

Thermal motion of the target nuclei causes Doppler broadening of the resonance peaks observed in the laboratory system: As the target temperature increases, the peaks become broader while their areas remain constant. This changes the average scattering, capture and fission rates and the whole neutron balance in a fission reactor. As a consequence the safety characteristics of the various fission reactor designs depend crucially on the cross section resonances of the main fuel constituents and in particular on their Doppler broadening. The Doppler effect is the only natural phenomenon that promptly counteracts a sudden power excursion in a fission reactor. Thermal expansion has the same tendency but is much slower. Quite generally one demands that the temperature rise accompanying a power excursion must result in less neutrons produced per neutron absorbed so that the fission chain reaction does not get out of hand. In more technical terms the prompt Doppler coefficient of reactivity (cf. e. g. Hummel and Okrent 1970) must be negative.

In shielding applications the minima displayed by the scattering and hence also by the total cross section (the sum of all partial cross sections for scattering, capture, fission etc.) provide dangerous energy "windows" for neutrons. In fusion reactor designs such as NET (Next European Torus) or ITER (International Thermonuclear Experimental Reactor), at present on the drawing boards, steel shielding is foreseen for the superconducting magnet coils. The windows in the total cross sections of the main steel components limit the efficiency of the shielding seriously (see Fig. 2 for ^{56}Fe).

These examples should suffice to illustrate the importance of neutron resonances for safety issues in nuclear technology. The topic of neutron resonance cross sections has been reviewed at Trieste before (Fröhner 1978, 1989) with the emphasis on analysis and critical evaluation of experimental resonance data. The present, shorter, treatment will emphasise

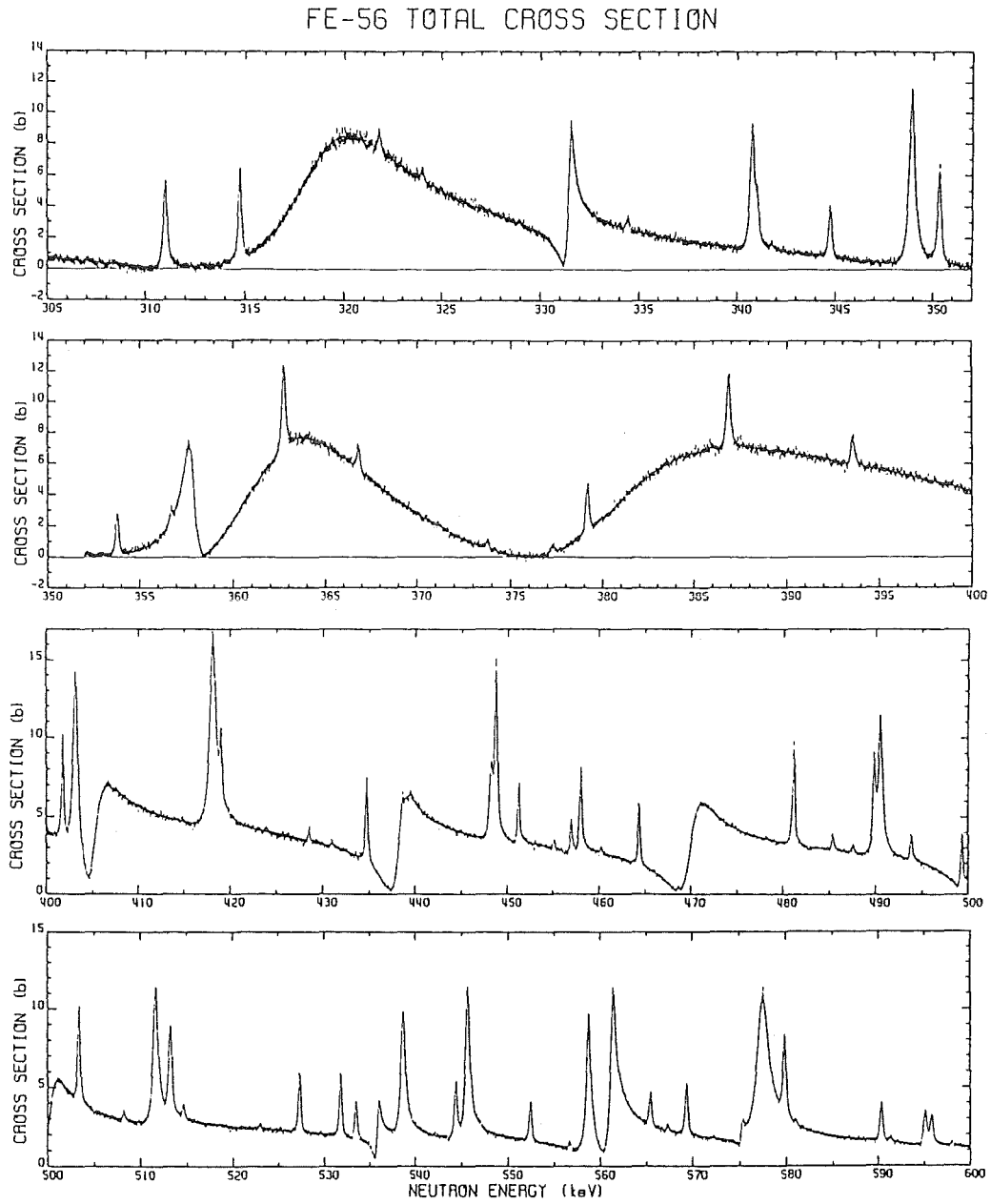

Fig. 2. Total cross section data for ^{56}Fe+n from 305 to 600 keV (bars) and resonance-theoretical fit (solid line, barely visible) with the one-channel Reich-Moore formalism of R-matrix theory. The broad asymmetric peaks are s-wave resonances, the narrow symmetric peaks are p- and d-wave resonances. The data were obtained in a time-of-flight transmission measurement with 201.6 m flight path at the Oak Ridge Electron Linear Accelerator. (From Perey et al. 1990)

safety-related aspects but by necessity much of the same ground will be covered again, in particular the basic theory.

2. Resonance Theory for the Resolved Region

Resolved resonances are described most conveniently by R-matrix theory. It attained its standard form more than thirty years ago with the comprehensive review article of Lane and Thomas (1958). This article is required reading for each specialist in the field. Briefly the principles of R-matrix theory are as follows. All collisions are considered as binary, an ingoing wave function describing the two incident particles, an outgoing wave function the two emerging reaction products. The incident particles could be, for instance, a neutron and a ^{235}U nucleus, the reaction products could be two fission fragments, of an excited ^{236}U nucleus and a photon, or a ^{235}U nucleus in its ground state and an elastically scattered neutron. Since the nuclear forces have short range but are not well understood otherwise, one divides configuration space into (i) an external region, where nuclear forces are negligible so that the well known wave functions for free or at most electromagnetically interacting particles can be used, and (ii) an internal region, where nuclear forces predominate. Although the internal wave function is unknown, it can at least be written as a formal expansion in terms of the eigenfunctions of an eigenvalue problem. This eigenvalue problem is defined by the (nonrelativistic) Schrödinger equation with prescribed logarithmic derivatives of the eigenfunctions at the boundary between the two regions. Matching external and internal wave functions at the boundary, and demanding finite probabilities everywhere, one finds that for a given ingoing wave all outgoing waves, and hence all cross sections, are parametrised by the eigenvalues and eigenvector components of the problem. These can be identified with the energies and decay amplitudes of the quasi-stationary compound states. All this will be discussed in detail in Section 3 below.

Although the principles of resonance theory are quite simple, the general expressions can look rather formidable. We cannot present full derivations except for simplified cases, but these will be chosen so as to illustrate all the essential arguments, and to provide the understanding of the general results that is needed for practical applications. The basic reaction theory - see e. g. Lynn (1968) - will be assumed to be known but we shall not hesitate to retrace its most important parts. The practically useful variants are

- the Blatt-Biedenharn formalism
- " single-level Breit-Wigner approximation (SLBW)
- " multi-level " - " " (MLBW)
- " (multi-level) Adler-Adler "
- " (multi-level) Reich-Moore "

The first one is quite general. It shows how cross sections can be expressed in terms of the unitary, symmetric collision matrix (S matrix) with special emphasis on angular distributions and on particle spins. It can be combined with any of the other four which provide different approximations to the collision matrix.

2.1 The Blatt-Biedenharn Formalism

Our notation in this and the following subsections will be basically that of Lane and Thomas (1958). We recall that in nuclear reaction theory one talks about reaction channels. Each channel is fully specified by

α, the partition of the compound system into reaction partners,
e. g. ^{235}U + n or ^{236}U + γ (both involving the same compound nucleus)
J, the total angular momentum in units of $\hbar$,
ℓ, " orbital " " " " " $\hbar$,
s, " channel spin " " " $\hbar$.

The angular momenta satisfy the quantum-mechanical triangle relations

$$\vec{J} = \vec{\ell} + \vec{s}, \qquad \text{i.e.} \qquad |\ell - s| \leq J \leq \ell + s, \tag{1}$$

$$\vec{s} = \vec{I} + \vec{i}, \qquad \text{i.e.} \qquad |I - i| \leq s \leq I + i, \tag{2}$$

where $\vec{I}$ and $\vec{i}$ are the spins (in units of $\hbar$) of the two collision partners. Total energy, total angular momentum and (for all practical purposes) parity are conserved in nuclear reactions.

We further remember that for spinless, neutral particles one can solve the nonrelativistic Schrödinger equation for the boundary condition "stationary ingoing plane wave + stationary outgoing spherical wave" with the result

$$d\sigma_{\alpha\alpha} = \pi \lambda\!\!\!^{-2}_{\alpha} \Big| \sum_{\ell=0}^{\infty} (2\ell + 1)(1 - U_\ell) P_\ell(\cos\vartheta) \Big|^2 \frac{d\Omega}{4\pi} \tag{3}$$

for the differential elastic-scattering cross section, where the de Broglie wave length $2\pi\lambda\!\!\!^{-}_{\alpha} = \hbar/(\mu_\alpha v_{rel})$ corresponds to the relative motion of the collision partners, with reduced mass μ_α and relative speed v_{rel}. The angular-momentum eigenfunctions P_ℓ are Legendre polynomials of order ℓ. The sum terms with $\ell = 0, 1, 2, \ldots$ are said to belong to the s-, p-, d-, f- ... wave, a historical nomenclature taken over from atomic spectroscopy (where it refers to the so-called sharp, principal, diffuse, fundamental series of spectral lines). The collision function U_ℓ describes the modification of the ℓ-th outgoing partial wave relative to the case without interaction. Its absolute value gives the reduction in amplitude, its argument the phase shift caused by the interaction. With $P_\ell P_{\ell'} = (\ell\ell' 00, L0)^2 P_L$, where $(\ell\ell' 00, L0)$ is a Clebsch-Gordan coefficient vanishing unless $|\ell - \ell'| \leq L \leq \ell + \ell'$ and $(-)^{\ell+\ell'} = (-)^L$, one can write the differential cross section as a linear expansion in Legendre polynomials,

$$d\sigma_{\alpha\alpha} = \lambda\!\!\!^{-2} \sum_{L=0}^{\infty} B_L P_L(\cos\vartheta) d\Omega\,, \tag{4}$$

with coefficients

$$B_L = \frac{1}{4} \sum_{\ell,\ell'} (2\ell + 1)(2\ell' + 1)(\ell\ell' 00, L0)^2 (1 - U_\ell^*)(1 - U_{\ell'})\,. \tag{5}$$

Blatt and Biedenharn (1952) worked out the generalisation for particles with spin and for partition-changing (rearrangement) collisions. For zero Coulomb interaction they obtained

$$d\sigma_{\alpha\alpha'} = \frac{\lambda\!\!\!^{-2}}{(2i + 1)(2I + 1)} \sum_{s,s'} \sum_{L=0}^{\infty} B_L(\alpha s, \alpha' s') P_L(\cos\vartheta) d\Omega\,, \tag{6}$$

with coefficients

$$B_L(\alpha s,\alpha' s') = \frac{(-)^{s-s'}}{4}\sum_{J_1,J_2}\sum_{\ell_1,\ell_2}\sum_{\ell_1',\ell_2'}\bar{Z}(\ell_1 J_1 \ell_2 J_2, sL)\bar{Z}(\ell_1' J_1 \ell_2' J_2, s' L)$$
$$\times(\delta_{\alpha\alpha'}\delta_{\ell_1\ell_1'}\delta_{ss'} - U^{J_1}_{\alpha\ell_1 s,\alpha'\ell_1' s'})^*(\delta_{\alpha\alpha'}\delta_{\ell_2\ell_2'}\delta_{ss'} - U^{J_2}_{\alpha\ell_2 s,\alpha'\ell_2' s'}), \qquad (7)$$

$$\bar{Z}(\ell_1 J_1 \ell_2 J_2, sL) = \sqrt{(2\ell_1+1)(2\ell_2+1)(2J_1+1)(2J_2+1)}$$

$$\times(\ell_1\ell_2 00, L0)\, W(\ell_1 J_1 \ell_2 J_2, sL), \qquad (8)$$

where $W(\ell_1 J_1 \ell_2 J_2, sL)$ is a Racah coefficient, see e. g. Fano and Racah (1959) or de-Shalit and Talmi (1963). Our phase convention is that of Lane and Thomas (1958); a slightly different convention is used in the Z tables of Biedenharn (1953). The Z coefficients vanish unless the quantum-mechanical triangle relations for the vector sums,

$$\vec{\ell_1} + \vec{\ell_2} = \vec{L} = \vec{\ell_1'} + \vec{\ell_2'} \qquad (9)$$
$$\vec{\ell_i} + \vec{s} = \vec{J_i} = \vec{\ell_i'} + \vec{s'} \qquad (i = 1,2) \qquad (10)$$

are fulfilled. Parity conservation demands $(-)^{\ell}\Pi_\alpha = \Pi_i = (-)^{\ell'}\Pi_{\alpha'}$, where $\Pi_\alpha, \Pi_{\alpha'}$ are the eigenparities of the ingoing and outgoing particles (positive for neutrons, protons, α-particles and photons) and Π_i is the parity of the compound system with total angular momentum J_i (i = 1,2). If there is Coulomb interaction between the collision partners additional terms must be included, see Lane and Thomas (1958).

Let us integrate Eq. 6 over angles. Because all terms with $L < 0$ vanish because of the orthogonality of the P_L and because of

$$\bar{Z}(\ell_1 J_1 \ell_2 J_2, s0) = (-)^{J_1+s}\sqrt{2J_1+1}\,\delta_{J_1 J_2}\delta_{\ell_1\ell_2} \qquad (11)$$

- see de-Shalit and Talmi (1963) - one finds

$$\sigma_{\alpha\alpha'} = \pi\lambda_\alpha^2 \sum_J g_J \sum_{\ell,\ell'}\sum_{s,s'}\left|\delta_{\alpha\alpha'}\delta_{\ell\ell'}\delta_{ss'} - U^J_{\alpha\ell s,\alpha'\ell' s'}\right|^2, \qquad (12)$$

where

$$g_J \equiv \frac{2J+1}{(2i+1)(2I+1)} \qquad (13)$$

is the so-called spin factor.

We cannot go into the details of angular distributions but we do point out that they show interference between different partial waves, e. g. s and p wave, whereas angle-integrated cross sections do not. The latter are simple sums over terms with given ℓ and s, without cross terms, see Eq. 12. Nevertheless, a certain connexion exists between different partial waves. As already mentioned, the compound system and its quasi-stationary states are characterised, apart from energy, by total angular momentum, J, and parity, Π. Table 1 shows, for given target spin and positive parity, the possible combinations of ℓ, s and J for incident particles with spin $i = 1/2$. Certain $J\Pi$ combinations can be formed through

Table 1. Possible combinations of target spin I, orbital angular momentum ℓ and channel spin s resulting in total spin J, parity Π and spin factor g, for positive target parity Π_0 and projectile spin $i = 1/2$. (For negative parity all signs must be reversed.)

$I\Pi_0$	ℓ	s	$J\Pi$	g	$\sum g$	wave
0+	0	1/2	1/2+	1	1	s
	1	1/2	1/2-, 3/2-	1, 2	3	p
	2	1/2	3/2+, 5/2+	2, 3	5	d
			etc.			
1/2+	0	0	0+	1/4	1	s
		1	1+	3/4		
	1	0	1-	3/4	3	p
		1	0-, 1-, 2-	1/4, 3/4, 5/4		
	2	0	2+	5/4	5	d
		1	1+, 2+, 3+	3/4, 5/4, 7/4		
			etc.			
1+	0	1/2	1/2+	1/3	1	s
		3/2	3/2+	2/3		
	1	1/2	1/2-, 3/2-	1/3 , 2/3	3	p
		3/2	1/2-, 3/2-, 5/2-	1/3 , 2/3 , 3/3		
	2	1/2	3/2+, 5/2+	2/3, 3/3	5	d
		3/2	1/2+, 3/2+, 5/2+, 7/2+	1/3, 2/3, 3/3, 4/3		
			etc.			

more than one channel if $\ell > 0$ and $I > 0$. If $I\Pi_0 = 1/2+$, for instance, resonances with $J\Pi = 1-$ can be excited by the two p waves with $s = 0$ and $s = 1$, and the 2+ levels can be excited by the d waves with $s = 0$ and $s = 1$. The neutron widths (that give the strength of the excitation, see below) for 1− and 2+ levels are therefore sums of two partial widths for the two channel spins. For $I\Pi_0 = 1+$ the 1/2+ levels can be excited even by partial waves with different ℓ, an s wave with $s = 1/2$ and a d wave with $s = 3/2$, while the 3/2+ levels are excitable by three partial waves, an s wave with $s = 3/2$ and two d waves with $s = 1/2$ and $s = 3/2$, and so on.

So we find that each quasi-stationary compound state shows up as a resonance in all open channels that are not excluded by the spin and parity selection rules. The intensities (peak areas) may differ, but the resonance width must be the same in all those channels, being proportional to the reciprocal half life of the compound state. In this context it should be understood that the customary terms s- or p-wave resonance actually mean that the level can be excited at least by the s or p wave but possibly also by higher-order partial waves with the same parity. To give an example the 3/2+ s-wave resonance resonances observed in neutron reactions with target nuclei with $I\Pi_0 = 1+$ contain also a d-wave component. It is true that at low incident energies the s-wave component is much larger because of the higher centrifugal barrier for d-wave neutrons (see below) but it must be realised that certain d, f, ... resonance sequences are masked by coinciding s, p, ... sequences. This is important e. g. for the statistical interpretation of observed level densities.

2.2 The Exact R-Matrix Expressions

The angle-integrated cross section $\sigma_{\alpha\alpha'}$, Eq.12, can be written as a sum over partial cross sections, $\sigma_{cc'}$, obtained by summing over all entrance channels $c \equiv \alpha J \ell s$ and exit channels $c' \equiv \alpha' J \ell' s'$ that lead from partition α to partition α'. In slightly simplified notation we write

$$\sigma_{cc'} = \pi \lambda\!\!\!^{-2}_c g_c |\delta_{cc'} - U_{cc'}|^2 . \tag{14}$$

Note that for $c \neq c'$ the partial cross section is proportional to the quantum-mechanical probability $|U_{cc'}|^2$ of a transition from channel c to channel c', and to the probability g_c of getting the correct angular momentum J from the spins of the collision partners. The Kronecker symbol $\delta_{cc'}$ arises since ingoing and outgoing particles cannot be distinguished if $c = c'$. The kinematical factor $\pi \lambda\!\!\!^{-2}_c$ relates probability and cross section. The collision matrix $\mathbf{U}$, often called scattering or S matrix, is symmetric because for all practical purposes we can consider nuclear (and Coulomb) interactions as invariant under time reversal. Moreover, $\mathbf{U}$ is unitary since the probabilities for transitions into the various channels must add up to unity, $\sum_{c'} |U_{cc'}|^2 = 1$. From the unitarity of $\mathbf{U}$ and Eq. 14 it follows that the total cross section for entrance channel c is a linear function of U_{cc},

$$\sigma_c \equiv \sum_{c'} \sigma_{cc'} = 2\pi \lambda\!\!\!^{-2}_c g_c (1 - \mathrm{Re}\ U_{cc}) . \tag{15}$$

The simplest expression is thus obtained for the total cross section, the most complicated one for elastic scattering (because of the Kronecker symbol). With a unitary collision matrix it is therefore more convenient to calculate σ_{cc} as the difference between σ_c and the other partial cross sections rather than directly from Eq. 14. The reciprocity relation between the cross sections for a reaction $c \rightarrow c'$ and the inverse reaction $c' \rightarrow c$,

$$\frac{\sigma_{c'c}}{g_{c'} \lambda\!\!\!^{-2}_{c'}} = \frac{\sigma_{cc'}}{g_c \lambda\!\!\!^{-2}_c} \tag{16}$$

follows immediately from the symmetry of $\mathbf{U}$.

These equations are quite general. In order to introduce resonances we invoke R-matrix theory which allows us to express $\mathbf{U}$ in terms of the channel matrix $\mathbf{R}$ (see Lane and Thomas 1958, Lynn 1968),

$$\begin{aligned} U_{cc'} &= e^{-i(\varphi_c + \varphi_{c'})} P_c^{1/2} \left\{ [\mathbf{1} - \mathbf{R}(\mathbf{L} - \mathbf{B})]^{-1} [\mathbf{1} - \mathbf{R}(\mathbf{L}^* - \mathbf{B})] \right\}_{cc'} P_{c'}^{-1/2} \\ &= e^{-i(\varphi_c + \varphi_{c'})} \left\{ \delta_{cc'} + 2i P_c^{1/2} [(\mathbf{1} - \mathbf{R}\mathbf{L}^\circ)^{-1} \mathbf{R}]_{cc'} P_{c'}^{1/2} \right\} , \end{aligned} \tag{17}$$

$$R_{cc'} = \sum_\lambda \frac{\gamma_{\lambda c} \gamma_{\lambda c'}}{E_\lambda - E} , \tag{18}$$

$$L^0_{cc'} \equiv L_{cc'} - B_{cc'} = (L_c - B_c)\delta_{cc'} \equiv (S_c + iP_c - B_c)\delta_{cc'} . \tag{19}$$

Alternatively the collision matrix can be expressed in terms of the level matrix $\mathbf{A}$,

$$U_{cc'} = e^{-i(\varphi_c + \varphi_{c'})} \left(\delta_{cc'} + i \sum_{\lambda,\mu} \Gamma^{1/2}_{\lambda c} A_{\lambda\mu} \Gamma^{1/2}_{\mu c'} \right) , \tag{20}$$

$$\Gamma^{1/2}_{\lambda c} \equiv \gamma_{\lambda c} \sqrt{2P_c} , \tag{21}$$

$$(\mathbf{A}^{-1})_{\lambda\mu} = (E_\lambda - E)\delta_{\lambda\mu} - \sum_c \gamma_{\lambda c} L_c^o \gamma_{\mu c} \,. \tag{22}$$

Note: Roman subscripts refer to reaction channels, Greek subscripts to compound levels, and **1** is the unit matrix. Three groups of physical quantities appear in these equations:

First, there are the resonance parameters, viz. formal level energies E_λ and probability amplitudes $\gamma_{\lambda c}$ for decay (or formation) of compound states λ via exit (or entrance) channels c, all neatly wrapped up in the R matrix (18), each level contributing one sum term (in terms of energies E a hyperbola). The $\gamma_{\lambda c}$ can be positive or negative, with practically random signs except near the ground state. Cross section formulae are usually written in terms of partial widths $\Gamma_{\lambda c}$ and total widths $\Gamma_\lambda \equiv \sum_c \Gamma_{\lambda c}$ rather than decay amplitudes.

The second group, hard-sphere phases φ_c and logarithmic derivatives L_c, depend only on the (known) in- and outgoing radial wave functions I_c and O_c at the channel radius a_c,

$$\varphi_c \equiv \arg O_c(a_c) = \text{arc tan}\, \frac{\text{Im } O_c(a_c)}{\text{Re } I_c(a_c)} \,, \tag{23}$$

$$L_c \equiv a_c \frac{O_c'(a_c)}{O_c(a_c)} = \left[r_c \frac{\partial \ln O_c}{\partial r_c} \right]_{r_c = a_c} . \tag{24}$$

The $S_c \equiv \text{Re } L_c$ are called shift factors for reasons that will become clear later on, the $P_c \equiv \text{Im } L_c$ are centrifugal-barrier penetrabilities.

The quantities B_c and a_c form the third group. They define the eigenvalue problem with eigenvalues E_λ. Their choice is a matter of convenience. The B_c are logarithmic derivatives of the radial eigenfunctions at the channel radii a_c. These radii define the boundary between the internal and the external region. They must be chosen so large that the nuclear interaction can be safely neglected if the distance r_c between the collision partners is larger, otherwise they are arbitrary. It is best to choose a_c just slightly larger than the radius of the compound nucleus (see Lynn 1968). A reasonable choice for neutron channels is $a_c = (1.23A^{1/3} + 0.80)$ fm, where A is the number of nucleons in the target nucleus. We mention here that in applied work all energies, resonance widths etc. are given in the laboratory system, as for instance in the widely used resonance parameter compilation of Mughabghab et al. (1981, 1984) known as the "barn book", or in computer files of evaluated nuclear data.

For neutral projectiles the outgoing radial wave functions are proportional to the spherical Hankel functions of the first kind, $h_\ell^{(1)}$,

$$O_c = I_c^* = ik_c r_c h_\ell^{(1)}(k_c r_c) \; \left(\simeq i^\ell e^{ik_c r_c} \quad \text{if} \quad k_c r_c \gg \sqrt{\ell(\ell+1)} \right) , \tag{25}$$

where $k_c = 1/\lambda\!\!\!^{-}_c$. The properties of the Hankel functions yield the recursion relations

$$L_0 = ik_c a_c = iP_0 \,, \qquad L_\ell = -\ell - \frac{(k_c a_c)^2}{L_{\ell-1} - \ell} \,, \tag{26}$$

$$\varphi_0 = k_c a_c \,, \qquad \varphi_\ell = \varphi_{\ell-1} - \arg(L_{\ell-1} - \ell) . \tag{27}$$

with which Table 2 is constructed. Note that $S_c = 0$ for $\ell = 0$, and that $S_c \to -\ell$ for $k_c a_c \to 0$ (at low energies). Therefore, $B_c = -\ell$ is a good choice for the resolved resonance region: It eliminates shift factors rigorously for s waves and, as we shall see

Table 2. Channel wave functions and related quantities for neutral projectiles ($\rho \equiv k_c r_c, \quad \alpha \equiv k_c a_c$)

ℓ	O_c	φ_c	S_c	P_c
0	$e^{i\rho}$	α	0	α
1	$e^{i\rho}\left(\frac{1}{\rho} - i\right)$	$\alpha - \arctan\alpha$	$\frac{-1}{\alpha^2+1}$	$\frac{\alpha^3}{\alpha^2+1}$
2	$e^{i\rho}\left(\frac{3}{\rho^2} - \frac{3i}{\rho} - 1\right)$	$\alpha - \arctan\frac{3\alpha}{3-\alpha^2}$	$\frac{-3(\alpha^2+6)}{\alpha^4+3\alpha^2+9}$	$\frac{\alpha^5}{\alpha^4+3\alpha^2+9}$
⋮	⋮	⋮	⋮	⋮

below, approximately also for higher-order partial waves. This means that the cross section peaks occur at the formal resonance energies E_λ as they should, instead of being shifted. S_c and P_c for photon and fission channels are usually taken as constant.

The basic resonance parameters E_λ, $\gamma_{\lambda c}$ depend on the unknown nuclear interaction. They can therefore not be calculated from first principles (except for simple models like a square well potential, see below). In typical applications of R-matrix theory they are just fit parameters, adjustable to experimental data. Depending on the choice of B_c they can be either real and constant or complex and energy-dependent.

The Wigner-Eisenbud version of R-matrix theory is obtained if the boundary parameters B_c are chosen as real constants (Wigner and Eisenbud 1947). The resonance parameters E_λ and $\gamma_{\lambda c}$ are then also real and constant, and the energy dependence of the collision matrix $\mathbf{U}$ is solely due to the φ_c and L_c, both known functions of $k_c a_c$, i. e. of energy. This makes the Wigner-Eisenbud version the most convenient formalism for most purposes. It is easily checked that the real R matrix yields a unitary collision matrix which means the partial cross sections add up to the total cross section, see Eq. 15. A certain problem is, however, the need to invert either the channel matrix $\mathbf{1} - \mathbf{RL}^\circ$ of Eq. 17, or the inverse level matrix $\mathbf{A}^{-1}$ of Eq. 22. Both matrices have very high rank. In practice the difficulty is overcome by various approximations to the inverse level matrix as will be shown below.

The Kapur-Peierls version of R-matrix theory is obtained with the choice $B_c = L_c$, i. e. $L_c^\circ = 0$ (Kapur and Peierls 1938). This removes the need for matrix inversion completely, since $\mathbf{1} - \mathbf{RL}^\circ = \mathbf{1}$, but leads to complex resonance parameters which depend implicitly on energy in a rather obscure way as now the very definition of the eigenvalue problem varies with energy, and thus the eigenvalues and the whole system of eigenfunctions, too. Moreover, the unitarity of the collision matrix is not manifest because the R matrix is complex. In spite of these handicaps formulae of the Kapur-Peierls type are useful in narrow energy ranges, in particular for the description of Doppler broadening. We shall

write the complex and energy-dependent Kapur-Peierls parameters as $\mathcal{E}_\lambda$, $g_{\lambda c}$ in order to distinguish them from the real and constant Wigner-Eisenbud parameters E_λ, $\gamma_{\lambda c}$. Thus

$$U_{cc'} = e^{-i(\varphi_c+\varphi_{c'})}\left(\delta_{cc'} + i\sum_\lambda \frac{G_{\lambda c}^{1/2} G_{\lambda c'}^{1/2}}{\mathcal{E}_\lambda - E}\right), \tag{28}$$

$$G_{\lambda c}^{1/2} = g_{\lambda c}\sqrt{2P_c}\,. \tag{29}$$

Note that the Kapur-Peierls form of the collision matrix (and hence the corresponding total cross section expression) involve a simple sum over levels, whereas the Wigner-Eisenbud expression (20) involves a double sum.

2.3 Illustration: R-Matrix Description of Single-Particle Interaction with Complex Potential (Spherical Optical Model)

The R-matrix equations reviewed so far are practically all that is needed in applied work from the whole apparatus of resonance theory. They ought to be thoroughly understood, however, and experience shows that this is not easy for the beginner. He might therefore wish to look at a simple illustration that shows the essential steps in the development of the theory and exhibits the meaning of the various quantities without the complications of spin algebra and matrix notation. Such an illustration is offered by the spherical optical model, with results of practical relevance for the unresolved resonance region.

2.3.1 Schrödinger Equation and Boundary Conditions

Consider spinless, neutral particles with mass m, interacting with a spherical, complex potential of finite range as shown in Fig. 3. From the Schrödinger equation

$$\left(\frac{-\hbar^2}{2m}\nabla^2 + V + iW\right)\psi = E\psi \tag{30}$$

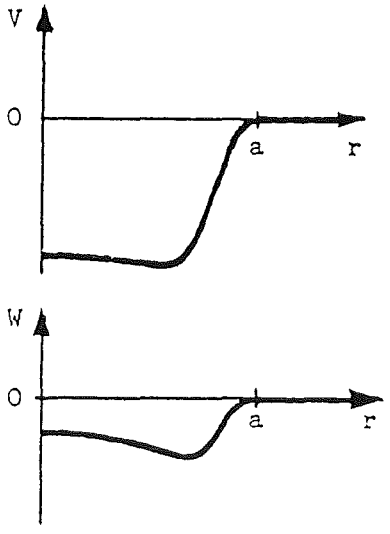

Fig. 3.

one finds, with the usual partial-wave expansion in Legendre polynomials, $\psi = \sum_\ell u_\ell(r)P_\ell(\cos\vartheta)/r$, and with $E = \hbar^2k^2/(2m)$, the radial wave equation

$$u_\ell'' + \left[k^2 - \frac{2m}{\hbar^2}(V+iW) - \frac{\ell(\ell+1)}{r^2}\right]u_\ell = 0\,. \tag{31}$$

The boundary conditions,

$$u_\ell(0) = 0\,, \tag{32}$$

$$u_\ell(r) = I_\ell(r) - U_\ell O_\ell(r) \quad \text{if} \quad r \geq a\,, \tag{33}$$

follow from the requirements that probabilities must remain finite and that beyond the range of the potential, $r > a$, one has ingoing and outgoing spherical waves I_ℓ, O_ℓ, the outgoing wave being modified relative to the case without interaction, by a complex factor, the collision function U_ℓ.

2.3.2 Orthogonal base in the internal region

Next we introduce for each channel ℓ a base of real, orthogonal functions $u_{\lambda\ell}$ for the interior region by demanding

$$u''_{\lambda\ell} + [k_\lambda^2 - \frac{2m}{\hbar^2}V - \frac{\ell(\ell+1)}{r^2}]u_{\lambda\ell} = 0\,, \qquad (r \le a) \tag{34}$$

$$u_{\lambda\ell}(0) = 0\,, \tag{35}$$

$$a\frac{u'_{\lambda\ell}(a)}{u_{\lambda\ell}(a)} = B_\ell\,. \tag{36}$$

Here we see the meaning of the boundary parameter B_ℓ: It is the prescribed logarithmic derivative of the internal eigenfunction at the boundary, to be compared with the similar definition of L_ℓ in terms of the external wave function, Eq. 24. Since we omitted the imaginary part of the potential in the wave equation (34) everything becomes real, including the eigenfunctions, if we choose B_ℓ real. (Similarly the self-adjoint Hamiltonian of the general theory has real eigenfunctions for real B_c.) The orthogonality of the eigenfunctions is readily checked as follows. The wave equation (34) yields

$$\begin{aligned}\int_0^a dr\,(u''_{\lambda\ell}u_{\mu\ell} - u_{\lambda\ell}u''_{\mu\ell}) &= (k_\mu^2 - k_\lambda^2)\int_0^a dr\,u_{\lambda\ell}u_{\mu\ell} \\ &= u'_{\lambda\ell}(a)u_{\mu\ell}(a) - u_{\lambda\ell}(a)u'_{\mu\ell}(a)\,.\end{aligned} \tag{37}$$

(The integration by parts leading to the last expression corresponds to application of Green's theorem in the general R-matrix theory.) The last expression vanishes because of the boundary condition (36). Thus we have orthogonality,

$$\int_0^a dr\,u_{\lambda\ell}u_{\mu\ell} = a\delta_{\lambda\mu} \tag{38}$$

The normalisation constant a is arbitrary but ensures the correct dimension.

2.3.3 Surface Equation

We can now expand the (unknown) internal wave function at least formally in terms of the internal eigenfunctions,

$$u_\ell = \sum_\lambda c_{\lambda\ell}u_{\lambda\ell} \qquad (r \le a), \tag{39}$$

$$c_{\lambda\ell} = \frac{1}{a}\int_0^a dr\,u_{\lambda\ell}u_\ell\,. \tag{40}$$

More specific information about the last integral, i. e. about the expansion coefficients, can be obtained from the wave equations and boundary conditions for $u_{\lambda\ell}$ and u_ℓ. We employ the same procedure that we have just applied to derive the orthogonality integral. From the wave equations (31) and (34) we get

$$\int_0^a dr\,(u''_\ell u_{\lambda\ell} - u_\ell u''_{\lambda\ell}) = (k_\lambda^2 - k^2 + i\frac{2m}{\hbar^2}\overline{W}_\lambda)\int_0^a dr\,u_\ell u_{\lambda\ell}\,, \tag{41}$$

where

$$\overline{W}_\lambda \equiv \frac{\int_0^a dr\, u_\ell u_{\lambda\ell} W}{\int_0^a dr\, u_\ell u_{\lambda\ell}} \tag{42}$$

is a volume average over the absorptive potential. Integrating by parts ("Green's theorem") and using the boundary conditions, Eqs. 32, 35 and 36, we find

$$[au'_\ell(a) - B_\ell u_\ell(a)]u_{\lambda\ell}(a) = \frac{2ma^2}{\hbar^2}(E_\lambda - E - i\overline{W}_\lambda)c_{\lambda\ell}\,, \tag{43}$$

where $E_\lambda \equiv \hbar^2 k_\lambda^2/(2m)$. Inserting $c_{\lambda\ell}$ from this equation in the expansion (39) we arrive at the "surface equation"

$$u_\ell = R_\ell(au'_\ell - B_\ell u_\ell) \qquad \text{for} \qquad r = a\,, \tag{44}$$

where the R function is defined by

$$R_\ell \equiv \sum_\lambda \frac{\gamma_{\lambda\ell}^2}{E_\lambda - E - i\Gamma_{\lambda a}/2} \tag{45}$$

with decay amplitudes

$$\gamma_{\lambda\ell} \equiv \sqrt{\frac{\hbar^2}{2ma^2}}u_{\lambda\ell}(a) \tag{46}$$

and an "absorption" width

$$\Gamma_{\lambda a} \equiv -2\overline{W}_\lambda\,. \tag{47}$$

The surface equation is analogous to the matrix equation $\mathbf{V} = \mathbf{R}(\mathbf{D} - \mathbf{BV})$ of the general theory that connects the "value" and "derivative" matrices $\mathbf{V}$ and $\mathbf{D}$ at the configuration space surface by means of the R matrix $\mathbf{R}$, given the diagonal matrix $\mathbf{B}$ of boundary parameters (see Lane and Thomas 1958). Eq. 46 shows that the decay amplitudes $\gamma_{\lambda\ell}$ are essentially the values of the radial eigenfunctions at the surface of the internal region.

2.3.4 Collision Function in Terms of the R Function

Our ultimate goal is an expression for the collision function (from which the cross sections can be calculated) free of the unknown internal functions u_ℓ and u'_ℓ. This is accomplished by matching the external and internal wave functions at the surface, $r = a$, which is surprisingly easy with the surface equation. We must only replace the unknown functions by the known in- and outgoing radial wave functions I_ℓ and O_ℓ with the help of the matching conditions

$$u_\ell = I_\ell - U_\ell O_\ell \qquad (r = a)\,, \tag{48}$$

$$au'_\ell = a(I'_\ell - U_\ell O'_\ell) = L_\ell^* I_\ell - U_\ell L_\ell O_\ell\,, \qquad (r = a) \tag{49}$$

and solve for U_ℓ. The result,

$$U_\ell = \frac{I_\ell}{O_\ell}\frac{1 - R_\ell(L_\ell^* - B_\ell)}{1 - R_\ell(L_\ell - B_\ell)} = e^{-2i\varphi_\ell}\left(1 + \frac{2iR_\ell P_\ell}{1 - R_\ell L_\ell^0}\right), \tag{50}$$

with the R function defined by Eq. 45, is the analogue of the general Eqs. 17, 18.

In contrast to the Wigner-Eisenbud R matrix, Eq. 18, our R function is complex due to the appearance of $i\Gamma_{\lambda a}/2$ in the denominators. It looks, in fact, exactly like the reduced R matrix of the Reich-Moore approximation to be discussed below, where $\Gamma_{\lambda a}$ will be seen to represent decays into a large number of "eliminated" channels. This approximation works well if the decay amplitudes of the eliminated channels are small but numerous, with random signs. The absorptive potential W of the optical model can therefore be interpreted as accounting for reactions leading from the (retained) elastic channels to other (eliminated) channels for processes such as (n,n'), (n,γ), (n,p), (n,2n) etc.

A more general connexion between the optical model and the theory of compound resonances emerges if we average the total cross section of the general theory, Eq. .15, over an energy interval that is so wide that it contains many resonances, yet so small that weak energy dependences (of $\lambda\!\!\!^{-} = 1/k, \varphi_\ell, L_\ell^0$ and of level statistics) can be neglected. For a heavy nucleus like ^{238}U these conditions are easily satisfied in the unresolved resonance region: An averaging interval at 100 keV, 5 keV wide, contains about 100 s-wave and 300 p-wave resonances, i. e. statistically meaningful samples. Averaging the total cross section means averaging the collision function, thanks to the linear relationship, Eq. 15. With a Lorentzian weight function centred at E and having width I (half width at half maximum) one can average by contour integration in the complex energy plane. This is easy because the collision matrix has no poles above the real axis. The result is that $\bar{U}_{cc}$ is equal to our optical-model collision function U_ℓ, Eq. 50, with R_ℓ replaced by R_{cc} evaluated at the complex energy $E + iI$ (and weak energy dependences neglected):

$$\bar{U}_{cc} = U_\ell(E), \qquad (51) \qquad R_\ell(E) = R_{cc}(E + iI) \qquad (52)$$

We arrive thus at the fundamental relationship between the optical model and resonance theory: The resonance-averaged total cross section can be identified with the total cross section calculated from a complex single-particle potential. One defines

$$R_{cc}(E + iI) \equiv R_c^\infty + i\pi s_c\,, \qquad (53)$$

where

$$s_c = \frac{\overline{\gamma_c^2}}{D_c}\,, \qquad (54) \qquad R_c^\infty(E) = \mathcal{P}\int_{-\infty}^{\infty} dE'\,\frac{s_c(E')}{E' - E} \qquad (55)$$

are called the pole strength and the distant-level parameter, respectively, D_c is the mean spacing of levels excited via channel c, and $\mathcal{P}$ denotes a Cauchy (principal value) integral. These results are valid to the extent that sums over levels can be approximated by integrals ($\sum_\lambda \ldots \to \int dE'\rho_c(E')\ldots$) involving the level density $\rho_c \equiv 1/D_c$, and that I can be treated as a small quantity. At low energies, $E \to 0$, the "potential" scattering observed between resonances is equal to that of an impenetrable ("hard") sphere with effective radius

$$R_c' = a[1 - (2\ell + 1)R_c^\infty]^{1/(2\ell+1)}\,. \qquad (56)$$

The strength function S_ℓ conventionally used in applied work is related to the pole strength s_c by

$$S_\ell = 2k_c a_c s_c \sqrt{1\mathrm{eV}/E}\,. \qquad (57)$$

(In principle the strength function for a nonspherical complex potential could also depend on J, but this dependence seems to be so weak that it can be neglected.) The effective radius is obtained, together with the resonance parameters, from resonance analyses, i. e. fits to measured cross section data in the resolved resonance region, and the statistics of the resonance parameters yields the strength function - at least for the s-wave, in favourable cases also for the p and d wave. For a recent illustration see the resonance analysis of ^{56}Fe data by Perey et al. (1990). On the other hand, effective radii and strength functions can also be calculated from a complex (optical-model) potential, as we have just seen.

2.3.5 Complex Square-Well Potential

For a little numerical exercise let us specialise to a three-dimensional complex square-well potential as shown in Fig. 4, with the same well radius, a, for both the real and the imaginary part.

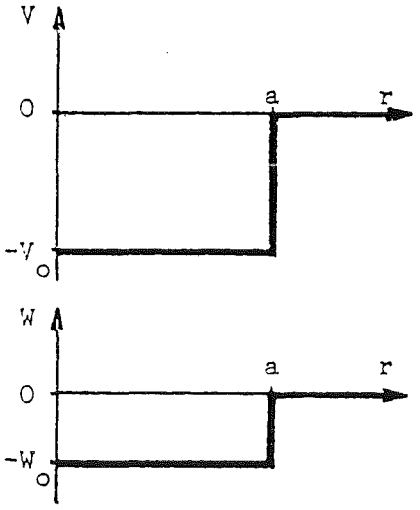

Fig. 4

The natural choice for the channel radii is $a_c = a$ for all channels. The internal radial eigenfunctions are now essentially spherical Bessel functions,

$$u_{\lambda\ell}(r) = K_\ell\, r j_\ell(K_\ell r)\,, \tag{58}$$

in particular

$$\begin{aligned} u_{\lambda 0}(r) &= \sin K_\lambda r\,, \\ u_{\lambda 1}(r) &= \frac{\sin K_\lambda r}{K_\lambda r} - \cos K_\lambda r\,, \\ &\vdots \end{aligned} \tag{58'}$$

with eigenvalues K_λ related to the eigenenergies E_λ by

$$K_\lambda^2 = \frac{2m}{\hbar^2}(E_\lambda - V_0)\,. \tag{58''}$$

For the eigenvalues one gets from Eq. 36

$$\text{for}\quad \ell = 0: \qquad B_0 \sin K_\lambda a \quad = K_\lambda a \cos K_\lambda a\,, \tag{59}$$

$$\text{for}\quad \ell \geq 1: \qquad B_\ell K_\lambda a\, j_\ell(K_\lambda a) = (K_\lambda a)^2\, j_{\ell-1}(K_\lambda a) - \ell\, K_\lambda a\, j_\ell(K_\lambda a)\,. \tag{59'}$$

The last equation follows from the recursion relations for spherical Bessel functions. We can simplify with the choice $B_\ell = -\ell$ which gives, with the normalisation of Eq. 38,

$$\begin{aligned} &\text{for } \ell = 0: && \cos K_\lambda a = 0, && E_\lambda = \Big(\frac{2\ell+1}{2}\pi\Big)^2 \frac{\hbar^2}{2ma^2} - V_0, && \gamma_{\lambda 0}^2 = \frac{\hbar^2}{2ma^2}\,, \\ &\text{for } \ell = 1: && \sin K_\lambda a = 0, && E_\lambda = (\lambda\pi)^2 \frac{\hbar^2}{2ma^2} - V_0, && \gamma_{\lambda 0}^2 = \frac{\hbar^2}{2ma^2}\,, \\ &\text{for } \ell = 2: && \tan K_\lambda a = 0, && \text{etc.} \end{aligned} \tag{60}$$

The decay amplitudes $\gamma_{\lambda\ell}$ for the square well are the same for all λ and ℓ, depending only on the well radius, and the absorption widths $\Gamma_{\lambda a} = -2W_0$ (cf. Eqs. 42 and 47) depend only on the depth of the imaginary well. The s- and p-wave eigenvalues correspond to simple ratios between the diameter of the square well, 2a, and the internal wave length, $\Lambda \equiv 2\pi/K$ (with $\hbar^2K^2/(2m) = E - V_0$),

$$\begin{aligned} &\text{for } \ell = 0: && 2a/\Lambda = 1/2,\ 3/2,\ 5/2, \ldots \\ &\text{for } \ell = 1: && 2a/\Lambda = 1,\ 2,\ 3, \ldots \end{aligned} \tag{61}$$

as might have been expected from an optical, i. e. wave-mechanical, model.

We can now calculate neutron strength functions and effective nuclear radii for a complex square well of reasonable size and depth, say

$$a = 1.35 \text{ fm } A^{1/3}, \qquad V_0 = 50 \text{ MeV}, \qquad W_0 = 3 \text{ MeV},$$

and compare them with values determined from resolved resonance data, which means at low energies ($E \simeq 0$). For $E = 0$ our square well model yields

$$R_\ell^\infty + i\pi s_\ell = \sum_\lambda \frac{\gamma_{\lambda\ell}^2 E_\lambda}{E_\lambda^2 + \Gamma_{\lambda a}^2/4} + i \sum_\lambda \frac{\gamma_{\lambda\ell}^2 \Gamma_{\lambda a}/2}{E_\lambda^2 + \Gamma_{\lambda a}^2/4}. \tag{62}$$

The main variation with nuclear radius (or nucleon number) comes from E_λ. Therefore the pole strength has maxima whenever one of the E_λ vanishes. According to Eq. 60 this happens under the conditions

$$\begin{aligned} &\text{for } \ell = 0: && a = \left(\lambda + \frac{1}{2}\right)\pi \frac{\hbar}{\sqrt{2mV_0}} \\ &\text{for } \ell = 1: && a = (\lambda + 1)\pi \frac{\hbar}{\sqrt{2mV_0}} \qquad \text{etc.} \end{aligned} \tag{63}$$

with $\lambda = 0, 1, 2, \ldots$ Table 3 lists the nucleon numbers at which size resonances should occur. Agreement with observed peak positions is not bad for our simple model, as can be seen from Fig. 5. The observed 4s peak, however, is split in two components which can be explained as due to nuclear deformation: The two components correspond to waves just fitting into the short and long axes of an ellipsoidal potential. The strength functions calculated from such a potential are also shown in the figure. Fig. 6 shows observed and calculated effective radii for the s-wave. The oscillations of the data around the curve $R' = 1.35$ fm $A^{1/3}$ reflect the behaviour of R_0^∞ indicated in Eq. 62. They are well reproduced by realistic optical-model calculations. It should be clear by now how optical-model potentials can be tested and improved with resolved-resonance data.

A convenient starting point for the practically important versions of R-matrix theory is the inverse level matrix. We shall consider the following representations and approximations.

Table 3. Size resonance positions for a complex square well with $a = 1.35$ fm $A^{1/3}$, $V_0 = -50$MeV, $W_0 = -3$MeV			
ℓ	Spectroscopic Symbol	Nucleon Number A at Peak	
		calculated	observed
0	2s	11	~ 11
	3s	52	~ 55
	4s	144	~ 160
1	2p	27	~ 25
	3p	90	~ 95
	4p	215	~ 240

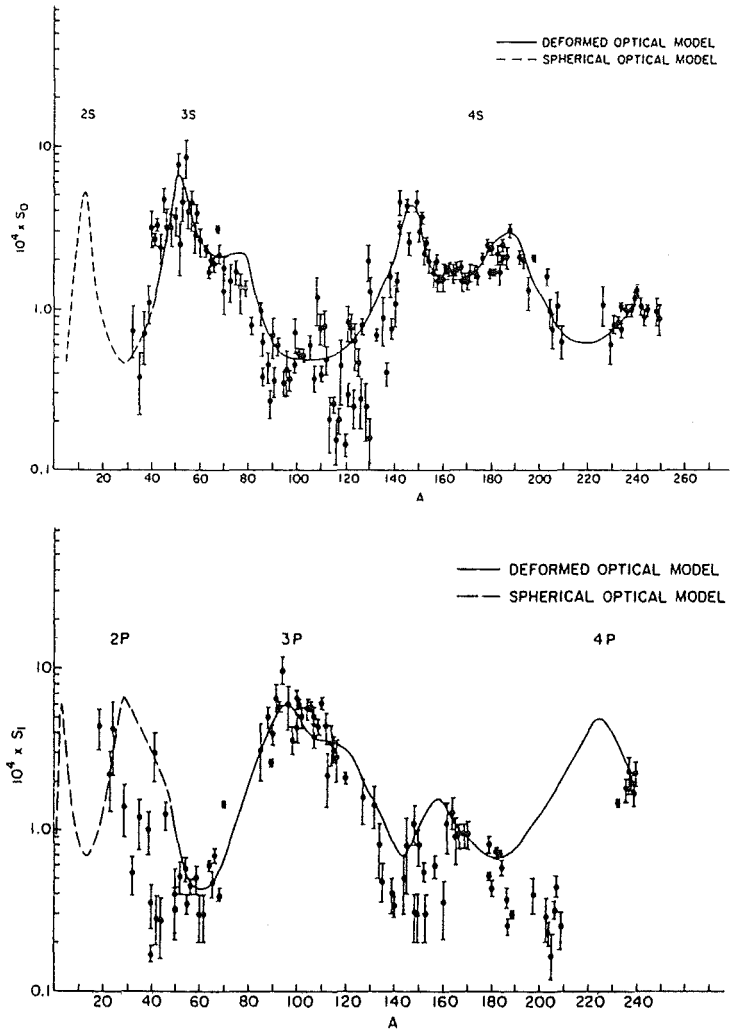

Fig. 5. Neutron strength functions obtained from resolved resonance data (point symbols) and from optical-model calculations (curves), for $\ell = 0$ (top) and $\ell = 1$ (bottom), from Mughabghab et al. (1984).

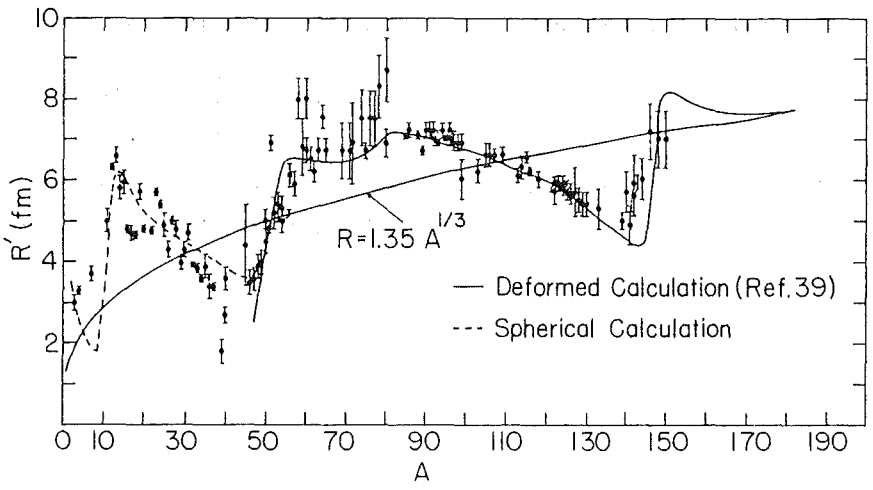

Fig. 6. Effective nuclear radii for s-wave neutron scattering, obtained from resolved resonance data (point symbols) and from optical-model calculations (curves), from Mughabghab et al. (1981).

Wigner-Eisenbud representation (exact)
with B_c real and constant:

$$(\mathbf{A}^{-}1)_{\lambda\mu} = (E_\lambda - E)\,\delta_{\lambda\mu} - \sum_c \gamma_{\lambda c} L_c^o \gamma_{\mu c} \tag{64}$$

(eigenvalues E_λ and decay amplitudes $\gamma_{\lambda c}$ real, constant, energy dependence of L_c^o known)

Kapur-Peierls representation (exact)
with $B_c = L_c$:

$$(\mathbf{A}^{-1})_{\lambda\mu} = (\mathcal{E}_\lambda - E)\,\delta_{\lambda\mu} \tag{65}$$

(eigenvalues $\mathcal{E}_\lambda$ and decay amplitudes $g_{\lambda c}$ complex, energy dependences implicit, obscure)

Single-level Breit-Wigner approximation (SLBW)
Only one level retained, all others neglected:

$$(\mathbf{A}^{-}1)_{\lambda\mu} \to E_0 - E - \sum_c L_c^o \gamma_c^2 \equiv E_0 + \Delta - E - i\Gamma/2 \tag{66}$$

(level shift Δ and total width $\Gamma = \sum_c \Gamma_c$ real, energy dependences explicit, well known)

Multi-level Breit-Wigner approximation (MLBW)
Off-diagonal elements of $\mathbf{A}^{-}1$ are neglected:

$$(\mathbf{A}^{-}1)_{\lambda\mu} = (E_\lambda - E - \sum_c L_c^o \gamma_{\lambda c}^2)\,\delta_{\lambda\mu} \equiv (E_\lambda + \Delta_\lambda - E - i\Gamma_\lambda/2)\,\delta_{\lambda\mu} \tag{67}$$

(level shift Δ_λ and total width $\Gamma_\lambda = \sum_c \Gamma_{\lambda c}$ real, energy dependences explicit, well known)

Reich-Moore approximation
Off-diagonal contributions from photon channels, $c \in \gamma$, are neglected:

$$(\mathbf{A}^{-}1)_{\lambda\mu} = (E_\lambda + \Delta_{\lambda\gamma} - E - i\Gamma_{\lambda\gamma}/2)\,\delta_{\lambda\mu} - \sum_{c\notin\gamma} \gamma_{\lambda c} L_c^o \gamma_{\mu c} \tag{68}$$

(real level shift $\Delta_{\lambda\gamma}$ from photon channels usually absorbed in real, constant E_λ, radiation width $\Gamma_{\lambda\gamma} = \sum_{c\in\gamma} \Gamma_{\lambda c}$ real, usually taken as constant; other energy dependences explicit)

Adler-Adler approximation
Energy dependence of L_c^o neglected:

$$(\mathbf{A}^{-}1)_{\lambda\mu} = (E_\lambda - E)\,\delta_{\lambda\mu} - \sum_{c} \gamma_{\lambda c} \sqrt{L_c^o(E_\lambda) L_c^o(E_\mu)}\,\gamma_{\mu c} \tag{69}$$

The Reich-Moore approximation is most, SLBW least accurate among these approximations. It should be realised that with a suitable choice of the boundary parameters the level shifts Δ_λ vanish at least locally. At low energies the best choice for neutron channels is $B_c = -\ell$ (see Table 1 and Appendix) as already mentioned. Note that the centrifugal-barrier penetrabilities P_c for neutrons, and hence all neutron widths,

$$\Gamma_{\lambda c}(E) \equiv 2P_\ell(E)\gamma_{\lambda c}^2 = \Gamma_{\lambda c}(|E_\lambda|)\frac{P_\ell(E)}{P_\ell(|E_\lambda|)} \qquad (c \equiv \{\alpha J \ell s\} \in n), \tag{70}$$

contain (at least) a factor $\sqrt{E}$. [The absolute values in this definition of the neutron width ensure applicability not only to compound states with $E_\lambda > 0$ but also to subthreshold ("negative", bound) states with $E_\lambda < 0$.] Additional factors in the p-, d-, ... penetrabilities behave for low energies as $E, E^2, \ldots$ As a consequence s-wave levels dominate at low energies while p-wave levels show up only at higher energies, d-wave levels at still higher energies, etc. The shifts and penetrabilities for photon and fission channels can usually be taken as constant. Hence these shifts vanish if we choose $B_c = S_c$, and the fission and radiation widths do not depend on energy. Let us now look at the cross section expressions resulting from the various representations and approximations.

2.4.1 Kapur-Peierls Cross Section Expressions

In anticipation of Doppler broadening we write the Kapur-Peierls collsion matrix (28) in the form

$$U_{cc'} = e^{-i(\varphi_c + \varphi_{c'})}\Big[\delta_{cc'} - \sum_\lambda \frac{G_{\lambda c}^{1/2} G_{\lambda c'}^{1/2}}{G_\lambda/2}(\psi_\lambda + i\chi_\lambda)\Big], \tag{71}$$

where the symmetric and asymmetric resonance profiles or line shape functions ψ_λ and χ_λ are defined by

$$\psi_\lambda + i\chi_\lambda \equiv \frac{iG_\lambda/2}{E - \mathcal{E}_\lambda} = \frac{G_\lambda^2/4}{(E-\tilde{E}_\lambda)^2 + G_\lambda^2/4} + i\frac{(E-\tilde{E}_\lambda)G_\lambda/2}{(E-\tilde{E}_\lambda)^2 + G_\lambda^2/4} \tag{72}$$

and the real Kapur-Peierls resonance energies $\tilde{E}_\lambda$ and widths G_λ by

$$\mathcal{E}_\lambda \equiv \tilde{E}_\lambda - iG_\lambda/2 . \tag{73}$$

The symmetric resonance profile is essentially (if we disregard the weak energy dependences of $\mathcal{E}_\lambda$ and of G_λ) a Lorentzian, and the asymmetric profile is its energy derivative. The resulting cross section expressions are

$$\sigma_c = 4\pi\lambda\!\!\!^{-2}_c g_c \Big\{ \sin^2\varphi_c + \mathrm{Re}\,\Big[e^{-2i\varphi_c}\sum_\lambda \frac{G_{\lambda c}}{G_\lambda}(\psi_\lambda + i\chi_\lambda)\Big]\Big\}, \tag{74}$$

$$\sigma_{cc'} = \sigma_c\delta_{cc'} - 4\pi\lambda\!\!\!^{-2}_c g_c\,\mathrm{Re}\,\Big[\sum_\lambda \frac{G^{1/2}_{\lambda c}G^{1/2}_{\lambda c'}}{G_\lambda} W_{cc'}(\mathcal{E}^*_\lambda)^*(\psi_\lambda + i\chi_\lambda)\Big], \tag{75}$$

$$W_{cc'}(\mathcal{E}^*_\lambda) \equiv \delta_{cc'} + i\sum_\mu \frac{G^{1/2}_{\mu c}G^{1/2}_{\mu c'}}{\mathcal{E}_\mu - \mathcal{E}^*_\lambda} . \tag{76}$$

The resonance profiles contain the rapid, resonance-related energy variations that are sensitive to Doppler broadening, while the other quantities vary slowly with energy. We stress that although the weak energy dependences of the Kapur-Peierls parameters are not known explicitly, the Kapur-Peierls formalism is exact.

2.4.2 SLBW Cross Section Expressions

The collision matrix for a single level,

$$U_{cc'} = e^{-i(\varphi_c + \varphi_{c'})}\Big(\delta_{cc'} + \frac{i\Gamma^{1/2}_c\Gamma^{1/2}_d}{E_0 + \Delta - E - i\Gamma/2}\Big), \tag{77}$$

is unitary. The resulting cross section expressions are

$$\sigma_c = 4\pi\lambda\!\!\!^{-2}_c g_c \Big\{ \sin^2\varphi_c + \frac{\Gamma_c}{\Gamma}(\psi\,\cos 2\varphi_c + \chi\,\sin 2\varphi_c)\Big], \tag{78}$$

$$\sigma_{cc'} = 4\pi\lambda\!\!\!^{-2}_c g_c \frac{\Gamma_c\Gamma_{c'}}{\Gamma}\,\psi \qquad (c \neq c'), \tag{79}$$

$$\sigma_{cc} = \sigma_c - \sum_{c'\neq c}\sigma_{cc'}, \tag{80}$$

with the resonance profiles given by

$$\psi + i\chi \equiv \frac{i\Gamma/2}{E - E_0 + i\Gamma/2} = \frac{\Gamma^2/4}{(E-E_0)^2 + \Gamma^2/4} + i\frac{(E-E_0)\Gamma/2}{(E-E_0)^2 + \Gamma^2/4} . \tag{81}$$

The basic resonance shape displayed by partial cross sections with $c \neq c'$ is essentially symmetric, wereas that of the total and of the scattering cross section is a sum of three terms: the nearly constant potential-scattering cross section, a symmetric resonance term, and an asymmetric term arising from interference between potential (hard-sphere) and

resonance scattering. It is easy to deduce from Eq. 78 that the total cross section reaches its peak value,

$$\sigma_c(E_+) = 4\pi\lambda\!\!\!^{-2}_c g_c \left(1 - \frac{\Gamma_a}{\Gamma}\cos^2\varphi_c\right), \tag{82}$$

at the energy

$$E_+ = E_0 + \frac{\Gamma}{2}\tan\varphi_c, \tag{83}$$

while the minimum value in the interference dip is

$$\sigma_c(E_-) = 4\pi\lambda\!\!\!^{-2}_c g_c \frac{\Gamma_a}{\Gamma}\sin^2\varphi_c = \frac{\Gamma_a}{\Gamma}\sigma_{p,c} \tag{84}$$

at

$$E_- = E_0 - \frac{\Gamma}{2}\cot\varphi_c, \tag{85}$$

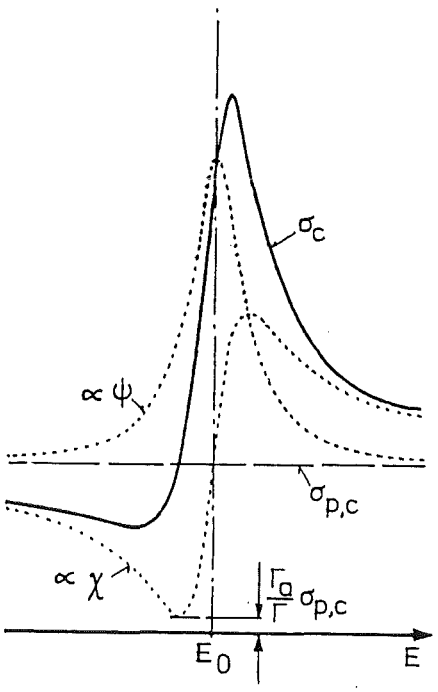

Fig. 7.

where $\Gamma_a \equiv \Gamma - \Gamma_n$ is the absorption width and $\sigma_{p,c}$ the potential-scattering cross section for entrance channel c. These last expressions are valid if the slow energy dependences of $\lambda\!\!\!^{-2}_c, \varphi_c$, Γ and Γ_n are negligible. For pure elastic scattering ($\Gamma_a = 0$) the minimum cross section is zero, the peak cross section is equal to the unitarity limit $4\pi\lambda\!\!\!^{-2}_c g_c$ (compare Eq. 15). The spin factor, hence the level spin J, can thus often be obtained by just measuring the resonance height. This works best for light nuclei or structural materials such as ^{56}Fe and other iron, nickel and chromium isotopes that are almost pure scatterers, and for broad, "isolated" resonances that are virtually unaffected by Doppler broadening and multi-level interference, and observable with good instrumental resolution. The depth of the interference minimum, most important for shielding calculations, is essentially given by the ratio Γ_a/Γ times the potential scattering cross section. At low energies s-wave reactions dominate, the potential scattering cross section is practically equal to $4\pi R'^2_c g_c$, i.e. constant (R'_c is the effective scattering radius, Eq. 56), while the capture and fission cross sections behave like $1/v$. This low-energy behaviour is quite generally true, not just in SLBW approximation.

Because of the slow variation of the sines and cosines with energy the total cross section resonances look differently at different energies: At low energies they look as in Fig. 7, with the interference minimum ("window") on the low-energy side. This shape is typical for the resolved region. At higher energies the symmetric term becomes less and less important until the asymmetric term dominates. At still higher energies, when $\varphi_c \approx \pi$, resonances appear as dips rather than peaks, and eventually the interference windows reappear on the high-energy side of the peaks.

In practice one must, however, describe cross sections with many resonances. One can simply add SLBW resonance terms (and add potential scattering for σ_c and σ_{cc}). This is the SLBW definition of the ENDF format (cf. Rose and Dunford 1990) that is used world-wide for applications-oriented, computer-readable libraries of evaluated neutron data. Since this ad-hoc recipe does not originate from a unitary collision matrix the unitarity constraint $0 < \sigma_c < 4\pi\lambda\!\!\!^{-2}_c g_c$ is not guaranteed. In fact, this "many-level" SLBW approximation is notorious for the occurence of nonphysical negative total and scattering cross sections. The reason is easy to understand: At low energies negative contributions can only come from the asymmetric profiles of resonances above. On average they are compensated by positive contributions from resonances below, but if the resonances above are unusually strong or those below unusually weak, scattering cross sections can become negative in the interference minima. Less noticeable but often equally bad is the opposite effect: SLBW peak cross sections can exceed the unitarity limit if resonances above are weak or those below strong.

2.4.3 MLBW Cross Section Expressions

The MLBW approximation is better than the many-level SLBW approximation. The collision matrix following from Eq. 67,

$$U_{cc'} = e^{-i(\varphi_c + \varphi_{c'})}\Big(\delta_{cc'} + i\sum_\lambda \frac{\Gamma_{\lambda c}^{1/2}\Gamma_{\lambda c'}^{1/2}}{E_\lambda + \Delta_\lambda - E - i\Gamma_\lambda/2}\Big)\,, \tag{86}$$

involves a simple sum over resonances, as the Kapur-Peierls collision matrix does. It follows that we can take over the Kapur-Peierls expressions with the replacements $E'_\lambda \to E_\lambda + \Delta_\lambda$, $G_\lambda \to \Gamma_\lambda = \sum_c \Gamma_{\lambda c}$, $G_{\lambda c}^{1/2} \to \Gamma_{\lambda c}^{1/2}$, whence

$$\sigma_c = 4\pi\lambda\!\!\!^{-2}_c g_c\Big[\sin^2\varphi_c + \sum_c \frac{\Gamma_{\lambda c}}{\Gamma_\lambda}(\psi_\lambda \cos 2\varphi_c + \chi_\lambda \sin 2\varphi_c)\Big]\,, \tag{87}$$

$$\sigma_{cc'} = \sigma_c\delta_{cc'} - 4\pi\lambda\!\!\!^{-2}_c g_c\,\mathrm{Re}\,\Big[\sum_\lambda \frac{\Gamma_{\lambda c}^{1/2}\Gamma_{\lambda c'}^{1/2}}{\Gamma_\lambda} W_{cc'}(\mathcal{E}_\lambda^*)^*(\psi_\lambda + i\chi_\lambda)\Big]\,, \tag{88}$$

$$W_{cc'}(\mathcal{E}_\lambda^*) = \delta_{cc'} + i\sum_\mu \frac{\Gamma_{\mu c}^{1/2}\Gamma_{\mu c'}^{1/2}}{E_\mu - E_\lambda - i(\Gamma_\mu + \Gamma_\lambda)/2}\,. \tag{89}$$

Since the partial cross sections (88) were derived from the collision matrix as absolute squares (see Eq. 14), they are guaranteed to be positive, and they are again linear functions of the line profiles ψ_λ and χ_λ defined exactly as in the SLBW case, Eq. 81. We recognise further that σ_c, Eq. 87, is just the "many-level" SLBW approximation. As the MLBW collision matrix is not unitary, however, σ_c is not the sum of the partial cross sections, Eq. 88. The MLBW approximation as defined in the ENDF format (cf. Rose and Dunford 1990) is even cruder, in fact it is an SLBW/MLBW hybrid: Only elastic scattering is actually calculated in MLBW approximation. All other partial cross sections are calculated in (many-level) SLBW approximation, and the total cross section as the sum over all

partials. This avoids negative cross sections yet prevents neither unphysical peak cross sections nor badly described interference minima for strongly overlapping levels. For light and medium-mass nuclei and for fissile actinides the MLBW approximation is therefore often inadequate, whereas it works quite well for compound systems with widely spaced, narrow levels like ^{232}Th + n or ^{238}U + n.

Note that the calculation of MLBW partial cross sections according to Eqs. 88 and 89 involves double sums over levels. Even with modern computers this can be time-consuming if hundreds of levels are to be included, as is not unusual with modern evaluated files. It is then better to calculate the partial cross section directly from the collision matrix (i. e. from Eqs. 14 and 86) which involves only a single sum over levels. For Doppler broadening, however, the representation (88), (89) in terms of line shape profiles has advantages as will be seen below.

2.4.4 Reich-Moore Cross Section Expressions

Usually very many photon channels contribute to the sum $\sum_c \gamma_{\lambda c} L_c^o \gamma_{\mu c}$ in the inverse level matrix $\mathbf{A}^{-1}$, Eq. 22. While their contributions all add up with the same sign in the diagonal elements, they tend to cancel in the off-diagonal elements because the decay amplitudes have practically random signs but comparable magnitudes. Therefore the error is quite small if one simply neglects all photon channel contributions to the off-diagonal elements, as proposed independently by Thomas (1955) and by Reich and Moore (1958). The resulting inverse level matrix, Eq. 68, belongs evidently to an eigenvalue problem with E_λ replaced by $E_\lambda - i\Gamma_{\lambda\gamma}/2$, with a "reduced" R matrix

$$R_{cc'} = \sum_\lambda \frac{\gamma_{\lambda c}\gamma_{\lambda c'}}{E_\lambda - E - i\Gamma_{\lambda\gamma}/2} \qquad (c, c' \notin \gamma), \tag{90}$$

reduced in the sense that it is defined in the subspace of nonphotonic channels only ($c \notin \gamma$). The only traces of the eliminated photon channels are the total radiation widths, $\Gamma_{\lambda\gamma}$, in the denominators. We recall that a similar complex R function was encountered in our R-matrix treatment of the optical model, which suggested that the imaginary part of the denominators in the reduced R matrix and the imaginary part of the complex potential are different consequences of the same phenomenon: absorption into compound states and subsequent decay into eliminated channels.

From the reduced R matrix one can calculate the reduced collision matrix and the cross sections for all retained channels. These matrices are usually of very low rank so that the inversion of $\mathbf{1} - \mathbf{RL}^o$ is easy. In fact, the highest rank employed in resonance analyses up to now is 3 (1 elastic, 2 fission channels). Cases with rank 2 involve 1 elastic plus 1 fission or 1 inelastic channel. For the overwhelming majority of neutron resonance data the only energetically allowed processes are merely elastic scattering and radiative capture, for which 1-channel Reich-Moore expressions without any matrices are sufficient, with R functions instead of R matrices. (We note that Fig. 2 shows an example of a 1-channel Reich-Moore fit.) The capture cross section can be found from

$$\sigma_{c\gamma} = \pi\lambda\!\!\!^{-2}_c g_c \sum_\lambda \Gamma_{\lambda\gamma} \left| \sum_{c' \notin \gamma} \frac{P_c^{1/2}[(\mathbf{1} - \mathbf{RL}^o)^{-1}]_{cc'} P_{c'}^{-1/2} \Gamma_{\lambda c'}^{1/2}}{E_\lambda - E - i\Gamma_{\lambda\gamma}/2} \right|^2 \tag{91}$$

(cf. Reich and Moore 1958). We note that the Reich-Moore approximation is exact in the limit of vanishing radiation widths (more precisely: vanishing widths for eliminated channels) in which it reduces to the general Wigner-Eisenbud formalism. It is also exact in the limit of one single level since in this case the Reich-Moore level matrix **A** reduces to the corresponding SLBW level matrix. Otherwise it is so exact that although the reduced collision matrix cannot be unitary - because of transitions into eliminated channels - the overall collision matrix can still be considered as unitary, i. e. as conserving probability flux, so that the capture cross section may alternatively be obtained as the difference

$$\sigma_{c\gamma} = \sigma_c - \sum_{c' \notin \gamma} \sigma_{cc'} \,, \tag{92}$$

with σ_c calculated from the reduced collision matrix element U_{cc} according to Eq. 15. Experience has shown that with this approximation all resonance cross section data can be described in detail, in the windows as well as in the peaks, even the weirdest multilevel interference patterns (see Fig. 2). It works equally well for light, medium-mass and heavy nuclei, fissile and nonfissile. It is often believed that the Reich-Moore approximation can only be applied to fissile nuclei, but actually the retained channels can be of any type - elastic, inelastic, fission, even individual photon channels such as those for transitions to the ground state or to specific metastable states. Furthermore, computer programs written for the Reich-Moore formalism can be used for general Wigner-Eisenbud R-matrix calculations - one must simply set all radiation widths (eliminated-channel widths) equal to zero.

One might expect that with all these advantages the Reich-Moore formalism is the most widely used one, but this is not true. The main reason is that the Reich-Moore cross sections cannot be expressed as sums over Breit-Wigner resonance profiles, at least not without some preparatory work. This is often considered as a disadvantage for Doppler broadening computations. We shall see below, however, that the problem is not as serious as some believe, and the general attitude among applications-oriented workers seems to change.

2.4.5 Adler-Adler Cross Section Expressions

The approximation (69) for the matrix $\mathbf{A}^{-1}$ is a generalisation for the s-wave expression used by Adler and Adler (1970), a generalistation that preserves symmetry with respect to the level indices λ and μ. Diagonalisation of the level matrix **A** yields the collision matrix in Kapur-Peierls form, Eqs. 28, 29, but with parameters $\mathcal{E}_\lambda$ and $g_{\lambda c}$ that do not depend on energy, in contrast to genuine Kapur-Peierls parameters. The corresponding cross section expressions are usually not written for specific channels (c, c',...) but for specific reaction types (x = f, γ, ..., total), restricted to $\ell = 0$:

$$\sigma \equiv \sum_{c \in n} \sigma_c = \sigma_p + \frac{1}{\sqrt{E}} \sum_\lambda \frac{1}{\nu_\lambda} \left(G_\lambda^{(T)} \psi_\lambda - H_\lambda^{(T)} \chi_\lambda \right) , \tag{93}$$

$$\sigma_x \equiv \sum_{c \in n} \sum_{c' \in x} \sigma_{cc'} = \frac{1}{\sqrt{E}} \sum_\lambda \frac{1}{\nu_\lambda} \left(G_\lambda^{(x)} \psi_\lambda - H_\lambda^{(x)} \chi_\lambda \right) , \qquad (x = \gamma, f, \ldots) , \tag{94}$$

where σ_p is the potential-scattering cross section, $G_\lambda^{(x)}/(\nu_\lambda \sqrt{E})$ and $H_\lambda^{(x)}/(\nu_\lambda \sqrt{E})$ are sums over all coefficients of ψ_λ and χ_λ in Eqs. 74-76, with $\nu_\lambda \equiv \Gamma_\lambda/2$ and $\sqrt{E}$ coming from

$P_c(E)$. The sums over λ are over levels irrespective of $J\Pi$, with spin factors absorbed in the coefficients $G_\lambda^{(x)}$ and $H_\lambda^{(x)}$. These coefficients, together with the level energies $\mu_\lambda \equiv E'_\lambda$, (half) widths ν_λ and the potential-scattering cross section σ_p (or an effective radius) are the Adler-Adler parameters. In principle one could define them even for isotopic mixtures, by similarly absorbing the relative abundances in the coefficients. The approximation (69) means essentially that the energy dependence of level shifts and total widths is neglected in the resonance denominators. Therefore the Adler-Adler approximation works well for fissile nuclei, for which $\Gamma_\lambda \approx \Gamma_{\lambda\gamma} + \Gamma_{\lambda f} = \text{const}$, but not so well for light or medium-mass nuclei, for which $\Gamma_\lambda \approx \Gamma_{\lambda n} = 2P_c(E)\gamma_{\lambda n}^2$.

2.4.6 Conversion of Wigner-Eisenbud to Kapur-Peierls Resonance Parameters

Wigner-Eisenbud parameters can be converted to Kapur-Peierls parameters as follows (Fröhner 1980). The collision matrix must be invariant under a change of boundary parameters, e. g. from $B_c = -\ell$ to $\tilde{B}_c = L_c^o$. (We shall use the tilde for Kapur-Peierls quantities.) From Eq. 17 we see that this implies $(\mathbf{1} - \mathbf{RL}^o)^{-1}\mathbf{R} = \tilde{\mathbf{R}}$, which with the abbreviations

$$\mathbf{K} \equiv \mathbf{L}^{o1/2}\mathbf{R}\mathbf{L}^{o1/2}, \qquad \tilde{\mathbf{K}} \equiv \mathbf{L}^{o1/2}\tilde{\mathbf{R}}\mathbf{L}^{o1/2} \tag{95}$$

yields

$$(\mathbf{1} - \mathbf{K})^{-1} = \mathbf{1} + \tilde{\mathbf{K}}. \tag{96}$$

The Kapur-Peierls resonance energies $\mathcal{E}_\lambda$ are the complex poles of $\tilde{\mathbf{K}}$, i. e. the solutions of

$$\det\left[\mathbf{1} - \mathbf{K}(\mathcal{E}_\lambda)\right] = 0 \tag{97}$$

because $\mathbf{A}^{-1} = \mathbf{C}[\mathbf{A}]/\det\mathbf{A}$ for any nonsingular matrix $\mathbf{A}$, where we use the notation $\det(\mathbf{A})$ for the determinant and $\mathbf{C}[\mathbf{A}]$ for the matrix of cofactors. The residues are obtained from Eq. 96. In the limit $E \to \mathcal{E}_\lambda$ one gets $[\mathbf{1} + \tilde{\mathbf{K}}(E)]_{cc'} \simeq L_c^{o\,1/2} g_{\lambda c} g_{\lambda c'} L_{c'}^{o\,1/2}/(E - \mathcal{E}_\lambda)$ on the right hand side, while on the left one has $\{\mathbf{C}[\mathbf{1}-\mathbf{K}(\mathcal{E}_\lambda)]\}_{cc'}/\det[\mathbf{1}-\mathbf{K}(\mathcal{E}_\lambda)]$, where Taylor expansion of the determinant gives $\det[\mathbf{1} - \mathbf{K}(E)] \simeq (E - \mathcal{E}_\lambda)\,\mathrm{tr}\,\{\mathbf{C}[\mathbf{1} - \mathbf{K}(\mathcal{E}_\lambda)]\,\mathbf{K}'(\mathcal{E}_\lambda)\}$. Hence the residues at the pole $\mathcal{E}_\lambda$ are

$$g_{\lambda c} g_{\lambda c'} = \frac{1}{\sqrt{L_c^o(\mathcal{E}_\lambda) L_{c'}^o(\mathcal{E}_\lambda)}} \frac{\{\mathbf{C}[\mathbf{1} - \mathbf{K}(\mathcal{E}_\lambda)]\}_{cc'}}{\mathrm{tr}\,\{\mathbf{C}[\mathbf{1} - \mathbf{K}(\mathcal{E}_\lambda)]\,\mathbf{K}'(\mathcal{E}_\lambda)\}}, \tag{98}$$

where tr denotes the trace and $\mathbf{K}'$ is the derivative of $\mathbf{K}$,

$$K'_{cc'}(E) = \frac{\partial}{\partial E} L_c^{o\,1/2} R_{cc'} L_{c'}^{o\,1/2} \simeq \sqrt{L_c^o(E) L_{c'}^o(E)} \sum_\mu \frac{\gamma_{\mu c}\gamma_{\mu c'}}{(E_\mu - E)^2}. \tag{99}$$

So we know how to calculate residuals from given poles, but how do we find the poles corresponding to given Wigner-Eisenbud parameters, i. e. how can we solve the deceptively simple-looking Eq. 97? Fortunately we know already the MLBW approximation $\mathcal{E}_\lambda \approx E_\lambda + \Delta_\lambda - i\Gamma_\lambda/2$, see Eq. 86. We may take it as an initial guess to be improved by iteration. In order to find an iteration scheme we write the determinant (86) in the form

$$\det(\mathbf{1} - \mathbf{K}) = 1 - \mathrm{tr}\;\mathbf{K} + F(\mathbf{K}), \tag{100}$$

where $-\mathrm{tr}\;\mathbf{K} + F(\mathbf{K})$ is the sum of $\det(-\mathbf{K})$ and all its principal minors (cf. e. g. Korn and Korn 1968), in particular

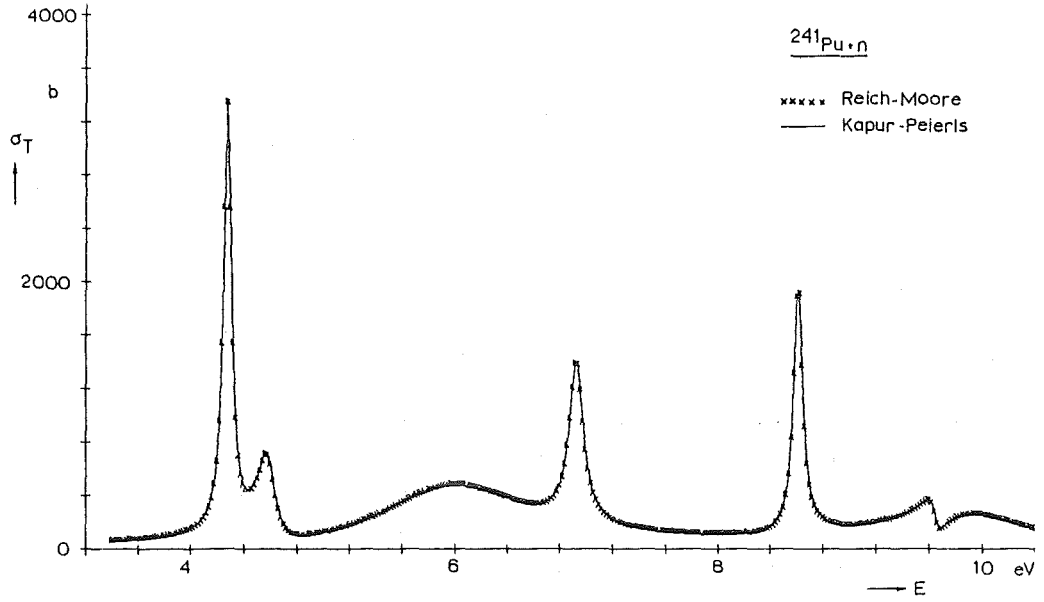

Fig. 8. Verification of the resonance parameter conversion technique explained in Subsect. 2.4.6: 3-channel Reich-Moore cross sections (symbols) and Kapur-Peierls cross sections calculated from converted resonance parameters (solid line) agree. (From Fröhner 1978)

$$
\begin{aligned}
&F = 0 && \text{for 1 (elastic) channel,}\\
&F = \det(-\mathbf{K}) && \text{for 2 channels,}\\
&F = \det(-\mathbf{K}) + \operatorname{tr} \mathbf{C}[-\mathbf{K}] && \text{for 3 channels.}
\end{aligned}
$$

Next we pull out the λ-th term of tr $\mathbf{K}$,

$$
\operatorname{tr} \mathbf{K}(\mathcal{E}_\lambda) = \sum_\mu \frac{1}{E_\mu - \mathcal{E}_\lambda} \sum_c L_c^o {\gamma_{\mu c}}^2 = \frac{\Delta_\lambda - i\Gamma_\lambda/2}{E_\lambda - \mathcal{E}_\lambda} + \sum_{\mu\neq\lambda} \frac{\Delta_\mu - i\Gamma_\mu/2}{E_\mu - \mathcal{E}_\mu}, \tag{101}
$$

which together with (100) permits us to rewrite (97) in the form

$$
\mathcal{E}_\lambda = E_\lambda + \frac{\Delta_\lambda - i\Gamma_\lambda/2}{1 + \sum_{\mu\neq\lambda} \frac{\Delta_\mu - i\Gamma_\mu/2}{E_\mu - \mathcal{E}_\lambda} + F(\mathcal{E}_\lambda)}. \tag{102}
$$

This equation is convenient for iteration: Inserting the initial MLBW approximation on the right-hand side one gets an improved value that can be reinserted on the right, and so on. After a few iterations the result becomes stable within some reasonable accuracy and can be inserted in (98) to yield the residues. Once all Kapur-Peierls parameters $\mathcal{E}_\lambda$ and $g_{\lambda c} g_{\lambda c'}$

are known one can insert them in the Kapur-Peierls cross section expressions that involve the resonance profiles.

Conversion of Reich-Moore to Kapur-Peierls parameters works in the same way, the only change being that E_μ must be replaced by $E_\mu - i\Gamma_{\mu\gamma}/2$, and Γ_μ by $\Gamma_\mu - \Gamma_{\mu\gamma}$ everywhere. Fig. 8 shows cross sections calculated from Reich-Moore parameters directly and from Kapur-Peierls parameters after conversion. Conversion of Wigner-Eisenbud to Adler-Adler parameters by matrix inversion is possible for instance with the POLLA code (de Saussure and Perez 1969).

2.4.7 Distant Levels

Modern evaluated nuclear-data libraries contain parameters for hundreds of resonances per isotope. Such large numbers suggest a statistical, average treatment of the more distant levels if a cross section is to be calculated at a given energy. Moreover, there are enormous numbers of unknown levels both below and above the resolved resonance region contributing noticeably to the R matrix, in particular near the edges of this region. In order to treat them at least statistically we split the (Reich-Moore) R matrix for a given level sequence (given $JI\!I$) into a distant-level and a local (known-level) term,

$$R_{cc'} = R^0_{cc'} + \sum_{\lambda=1}^{\Lambda} \frac{\gamma_{\lambda c}\gamma_{\lambda c'}}{E_\lambda - E - i\Gamma_{\lambda\gamma}/2}\,, \tag{103}$$

and replace the sums in the distant-level term by integrals,

$$\begin{aligned} R^0_{cc'} &= \Big(\sum_{\lambda} - \sum_{\lambda=1}^{\Lambda}\Big) \frac{\gamma_{\lambda c}\gamma_{\lambda c'}}{E_\lambda - E - i\Gamma_{\lambda\gamma}/2} \\ &\simeq \Big(\int_{-\infty}^{\infty} - \int_{\bar{E}-I/2}^{\bar{E}+I/2}\Big) \frac{dE'}{D_c} \langle\gamma_c\gamma_{c'}\rangle \frac{E' - E - i\bar{\Gamma}_\gamma/2}{(E'-E)^2 + \bar{\Gamma}_\gamma^2/4}\,, \end{aligned} \tag{104}$$

where $\bar{E}$ and I are midpoint and length of the interval containing the local (known) levels, $D_c = D_{c'} = D_J$ is the average level spacing, and $\bar{\Gamma}_\gamma$ the average radiation width. Especially for heavy nuclei the radiation width, as a sum over very many partial radiation widths, does not vary much from level to level so that $\Gamma_{\lambda\gamma} \simeq \bar{\Gamma}_\gamma$. Since $(E'-E)^2 \gg \bar{\Gamma}_\gamma^2/4$ for the distant levels we can neglect $\bar{\Gamma}_\gamma^2/4$ in the last expression. Moreover we can neglect the off-diagonal elements of the average matrix $\langle\gamma_c\gamma_{c'}\rangle$ because of the practically random signs of the $\gamma_{\lambda c}$. With our definition of pole strength s_c and distant-level parameters R_c^∞, Eqs. 54 and 55, we find in Reich-Moore approximation

$$R^0_{cc'} = \Big[R_c^\infty + 2s_c\Big(\text{ar tanh}\,\frac{E-\bar{E}}{I/2} + \frac{i\bar{\Gamma}_\gamma I/4}{I^2/4 - (E-\bar{E})^2}\Big)\Big]\delta_{cc'}\,. \tag{105}$$

The analogous distant-level contribution to the general Wigner-Eisenbud R matrix is obtained if one simply puts $\Gamma_{\lambda\gamma} = 0$ and $\bar{\Gamma}_\gamma = 0$ everywhere:

$$R^0_{cc'} = \Big[R_c^\infty + 2s_c\,\text{ar tanh}\frac{E-\bar{E}}{I/2}\Big]\delta_{cc'}\,. \tag{106}$$

We see that input from optical-model calculations (e. g. from Figs. 5 and 6) can be used to estimate the contribution of distant levels. If it is neglected, one gets edge effects near the boundaries of the range of local (known) levels. In order to speed up the calculation if very many resonances are given explicitly, one can retain only those in a certain range around the energy of interest, and let the others be described summarily by the distant-level part $\mathbf{R}^0$ of the R matrix. Experience shows that explicit inclusion of something like fifty levels below and fifty levels above the energy of interest ($I \approx 100\, D_c$) is enough for most purposes.

In Wigner-Eisenbud representation the effect of distant levels can be absorbed in the hard-sphere phases and resonance parameters: Since $\mathbf{R}^0$ is real and diagonal, the form of the equations is preserved if only the local levels are included in the R matrix but with the replacements

$$\varphi_c \to \varphi_c + \arg(1 - R^0_{cc} L^o_c), \tag{107}$$

$$\gamma_{\lambda c} \to \frac{\gamma_{\lambda c}}{|1 - R^0_{cc} L^o_c|} \equiv \alpha_{\lambda c}\,, \tag{108}$$

$$\gamma_{\lambda c} L^o_c \gamma_{\mu c} \to \alpha_{\lambda c}(L^o_c - R^0_{cc}|L^o_c|^2)\alpha_{\mu c}\,. \tag{109}$$

Our definition (56) of the effective nuclear radius can now be justified: At low energies, $E \to 0$, the replacement (107) is equivalent to replacement of the channel radius a_c by the effective radius R'_c in the original definition (23) of the hard-sphere phases, with R^0_{cc} evaluated at the midenergy, $E = \bar{E}$.

2.5 Doppler Broadening

In most practical applications resonance cross sections are needed in Doppler-broadened form. It is sometimes argued that for light nuclei Doppler broadening can be neglected. This may be true for the broad s-wave levels but certainly not for the narrow p-, d-, ... wave levels that in the case of the so-called structural materials (iron, nickel, chromium, cobalt, manganese etc.) contribute significantly to resonance absorption and activation.

2.5.1 Free-gas Approximation

Doppler broadening in nuclear reactions is caused by the thermal motion of target nuclei. Consider a parallel beam of monoenergetic particles with laboratory velocity $\vec{v}$, colliding with target nuclei whose velocities $\vec{u}$ are distributed in such a way that $p(\vec{u})d^3u$ is the fraction with velocities in a small three-dimensional region d^3u around $\vec{u}$ in velocity space. If ρ_1 and ρ_2 are the densities of beam and target particles, respectively, the number of reactions occurring per unit time and unit volume is

$$\rho_1\rho_2 \int d^3u\, p(\vec{u})\, |\vec{v} - \vec{u}|\, \sigma(|\vec{v} - \vec{u}|) \equiv \rho_1\rho_2 v \bar{\sigma}(v)\,, \tag{110}$$

where $\sigma(|\vec{v} - \vec{u}|)$ is the unbroadened cross section for a relative speed $|\vec{v} - \vec{u}|$ between the collision partners, and $\bar{\sigma}(v)$ the effective or Doppler-broadened cross section for incident particles with speed v. It is obvious from this definition that a $1/v$ cross section is not affected by Doppler broadening. Let us now assume that the target nuclei have the same velocity distribution as the atoms of an ideal gas, viz. the Maxwell-Boltzmann distribution

$$p(\vec{u})d^3u = \frac{1}{\pi^{3/2}} \exp\Big(-\frac{u^2}{u_T^2}\Big)\frac{d^3u}{u_T^3} \qquad \Big(\frac{M}{2}u_T^2 \equiv kT\Big)\,, \tag{111}$$

where M is the mass of the target nucleus and kT the gas temperature in energy units. Integrating over all possible relative velocities $\vec{w} \equiv \vec{v} - \vec{u}$ and employing polar coordinates with the polar axis parallel to the beam, $d^3u = d^3w = w^2 dw\, d\mu\, d\phi$ with $\mu = \cos\theta$, one finds easily the exact free-gas expression for the Doppler-broadened cross section (Solbrig 1961)

$$\bar{\sigma}(v) = \frac{1}{\sqrt{\pi}} \int_0^\infty \frac{dw}{u_T} \Big\{ \exp\Big[-\Big(\frac{w-v}{u_T}\Big)^2 \Big] - \exp\Big[-\Big(\frac{w+v}{u_T}\Big)^2 \Big] \Big\} \frac{w^2}{v^2} \sigma(w)$$
$$= \frac{1}{\sqrt{\pi}} \int_{-\infty}^\infty \frac{dw}{u_T} \exp\Big[-\Big(\frac{w-v}{u_T}\Big)^2 \Big] \frac{w|w|}{v^2} \sigma(|w|) . \qquad (112)$$

This means Gaussian broadening of the odd function $v|v|\sigma(|v|)$ on a speed scale ranging from $-\infty$ to $+\infty$, with a broadening width u_T. In terms of laboratory energies, $E = mv^2/2$, one has

$$\bar{\sigma}(E) = \frac{1}{\Delta\sqrt{\pi}} \int_0^\infty dE' \Big\{ \exp\Big[-\Big(\frac{E - \sqrt{EE'}}{\Delta/2}\Big)^2 \Big] - \exp\Big[-\Big(\frac{E + \sqrt{EE'}}{\Delta/2}\Big)^2 \Big] \Big\} \sqrt{\frac{E'}{E}} \sigma(E') , \qquad (113)$$

where

$$\Delta \equiv \sqrt{\frac{4EkT}{M/m}} \qquad (114)$$

is called the Doppler width. For $E \gg \Delta$, which is usually satisfied above a few eV, one can simplify by retaining only the first two terms of the expansion $\sqrt{EE'} = E + (E'-E)/2 + \ldots$ in the exponent, by neglecting the second exponential, and by shifting the lower limit of the integral to $-\infty$. The result is

$$\sqrt{E}\bar{\sigma}(E) = \frac{1}{\Delta\sqrt{\pi}} \int_{-\infty}^\infty dE' \exp\Big[-\Big(\frac{E' - E}{\Delta}\Big)^2 \Big] \sqrt{E'}\, \sigma(E') , \qquad (115)$$

which means Gaussian broadening of the reaction rate on the energy scale with a width Δ.

2.5.2 Cubic Crystal

Lamb (1939) found the expression (115) also for radiative capture of neutrons by the nuclei of a Debye crystal, in the practically most important case $\Gamma + \Delta > 4kT_D$, where T_D is the Debye temperature that is a measure of the binding force holding the atoms at their positions in the lattice, high for tightly bound and low for weakly bound atoms. The only difference between an ideal gas and a Debye crystal is that one must calculate the Doppler width not with the true temperature T but with an effective, "Lamb-corrected" temperature T_L given by

$$T_L = T\Big(\frac{T}{T_D}\Big)^3 \frac{3}{2} \int_0^{T_D/T} dx\, x^3 \coth\frac{x}{2} = T\Big(1 + \frac{1}{20}\frac{T_D^2}{T^2} - + \ldots\Big) \qquad (116)$$

that is usually - at room temperature - a few percent higher than T. With the theory of quasi-free scattering one finds the same result for scattering, and for cubic crystals in general. The correction as a function of T_D/T is given in curve form by Lamb (1939).

Problems with the Debye temperature of crystals containing both light and heavy nuclei are discussed by Lynn (1968).

2.5.3 Gaussian Broadening with Voigt Profiles

In Kapur-Peierls representation, Eqs. 74-76, all resonance cross sections appear as linear superpositions of symmetric and asymmetric line shape profiles (plus a slowly varying potential scattering cross section in case of σ_c and σ_{cc}). Since the shape profiles contain the rapid, resonance-type variations while everything else varies slowly we get Doppler-broadened cross section in good approximation if we simply replace the unbroadened ("natural") line shapes of the Kapur-Peierls expressions by the Gaussian-broadened profiles introduced by Voigt (1912)

$$\psi_\lambda = \frac{1}{\Delta\sqrt{\pi}} \int_{-\infty}^{\infty} dE' e^{-(E'-E)^2/\Delta^2} \frac{G_\lambda^2/4}{(E' - \tilde{E}_\lambda)^2 + G_\lambda^2/4}, \tag{117}$$

$$\chi_\lambda = \frac{1}{\Delta\sqrt{\pi}} \int_{-\infty}^{\infty} dE' e^{-(E'-E)^2/\Delta^2} \frac{(E' - \tilde{E}_\lambda)G_\lambda/2}{(E' - \tilde{E}_\lambda)^2 + G_\lambda^2/4}, \tag{118}$$

where Δ, $\tilde{E}_\lambda$ and G_λ are to be taken at $E' = E$. This means that all weak energy dependences are neglected locally, over the range (few Doppler widths) of the Gaussian weight function, but that their long-range effect is fully taken into account. Doppler broadening by means of the Voigt profiles is popular because fast subroutines are available for their computation (see e. g. Bhat and Lee-Whiting 1967). In Adler-Adler approximation their utilisation is straightforward. In other representations one must first convert from Wigner-Eisenbud to Kapur-Peierls parameters. In SLBW and MLBW approximation this is trivial, one has simply $\tilde{E}_\lambda = E_\lambda + \Delta_\lambda$, $G_{\lambda c}^{1/2} = \Gamma_{\lambda c}^{1/2}$, $G_\lambda = \Gamma_\lambda$ (cf. Eqs. 66, 67). In Reich-Moore approximation one must use iterative conversion as explained in Subsect. 2.4.6 which is easy to program and does not add significantly to computing time, especially if used with a fast algorithm for Gaussian broadening.

2.5.4 Gaussian Broadening with Turing's Method

A fast algorithm for Gaussian broadening of functions having poles in the complex plane (meromorphic functions) was proposed by Turing (1943). The combination $\psi + i\chi$ of natural resonance profiles is the simplest meromorphic function possible, with a single pole. So it is not surprising that Turing's method is widely used for the calculation of Voigt profiles. One introduces artificial, equidistant poles along the real axis and applies contour integration (see e.g. Bhat and Lee-Whiting 1967) to get

$$\begin{aligned}\psi + i\chi = &\frac{1}{\Delta\sqrt{\pi}} \sum_{n=-\infty}^{\infty} \delta E\, e^{-(E_n - E)^2/\Delta^2} \frac{i\Gamma/2}{E_n - E_0 + i\Gamma/2} \\ &+ \sqrt{\pi}\frac{\Gamma}{\Delta} \frac{e^{-(E - E_0 + i\Gamma/2)^2/\Delta^2}}{1 - e^{-2\pi i(E - E_0 + i\Gamma/2)/\delta E}} P + F,\end{aligned} \tag{119}$$

where δE is the (arbitrary) spacing of the artificial poles, $E_n = E + n\,\delta E$ is a grid point (artificial pole), and

$$P = \left\{ \begin{matrix} 0 \\ 1/2 \\ 1 \end{matrix} \right\} \qquad \text{for} \qquad \frac{\Gamma/2}{\Delta} \left\{ \begin{matrix} > \\ = \\ < \end{matrix} \right\}, \tag{120}$$

$$|F| \geq \frac{2}{\sqrt{\pi}} \Big[1 + \Big(\frac{E - E_0}{\Gamma/2} \Big)^2 \Big]^{1/2} \Big| 1 - \Big(\frac{2\pi\Delta^2}{\Gamma\,\delta E} \Big)^2 \Big|^{-1} \frac{e^{-(\pi\Delta/\delta E)^2}}{1 - e^{-2(\pi\Delta/\delta E)^2}} . \tag{121}$$

We recognise that Turing's approximation consists of (i) a simple sum approximation to the integral with bin width δE, (ii) a term involving the pole energy $E_0 + i\Gamma/2$ and a discontinuous factor P, and (iii) an error term F which becomes small for $\delta E < \Delta$ because of the factor $\exp[-(\pi\Delta/\delta E)^2]$. The pole term is a correction to the sum, needed only in the neighbourhood of narrow peaks (poles close to the real axis) for which the bin width of the sum approximation is too coarse, but negligible elsewhere as indicated by the factor P. With the choice $\delta E \simeq 0.7\Delta$ one can neglect the error term completely and still obtain relative accuracies of 10^{-7} or better (Bhat and Lee-Whiting 1967). Applying Turing's method to each term of the Kapur-Peierls cross section expressions (74) or (75) one finds

$$\begin{aligned} \sqrt{E}\bar{\sigma}(E) \simeq & \frac{1}{\Delta\sqrt{\pi}} \sum_{n=-N}^{N} \delta E\, e^{-(E_n - E)^2/\Delta^2} \sqrt{E_n}\sigma(E_n) \\ & + \pi\sqrt{E}\,\mathrm{Re} \sum_{\lambda} C_\lambda G_\lambda \frac{e^{-(E - \mathcal{E}_\lambda)^2/\Delta^2}}{1 - e^{-2\pi i(E - \mathcal{E}_\lambda)/\delta E}} P_\lambda , \end{aligned} \tag{122}$$

where C_λ is the coefficient of $\psi_\lambda + i\chi_\lambda$ in Eq. 74 (for total cross sections) or in Eq. 75 (for partial cross sections), and the factors P_λ are analogous to P, Eq. 120.

The first term on the right-hand side is again the sum approximation to the integral. Due to the rapidly decreasing weight in the wings of the Gaussian one needs only the sum terms with $-5 \leq n \leq +5$ for the usual accuracy of about 0.1% required in typical applications. Moreover, the natural (unbroadened) cross section $\sigma(E_n)$ can be calculated directly from the unconverted Wigner-Eisenbud or Adler-Adler parameters given in the evaluated files. Double sums are not needed: Natural MLBW cross sections are directly obtained from the collision matrix (86), Reich-Moore cross sections from the reduced R-matrix (90). In both cases one needs only single sums over levels. The computer time needed for the histogram approximation (first sum in Eq. 119) is therefore practically the same in all four approximations: SLBW, MLBW, Reich-Moore and Adler-Adler.

The pole term in Eq. 119, on the other hand, requires Kapur-Peierls parameters, but only for narrow resonances (nonvanishing P_λ) and only near their peaks where weak energy dependences can be neglected. Adler-Adler parameters need not be converted at all, for SLBW and MLBW the conversion is trivial. Only in Reich-Moore approximation must one convert by iteration as explained in Subsect. 2.4.6, but merely at few energies, namely at the formal resonance energies of the narrow resonances. The extra time needed for this preparation is only a small fraction of the total time required for comprehensive point cross section calculations for which time savings are important.

Turing's method can be applied, of course, not only to Gaussian broadening on the energy scale, Eq. 115, but also to Gaussian broadening on the speed (or momentum) scale with the free-gas kernel, Eq. 112. In the latter case there is even an extra bonus: The width of the Gaussian weight function does not depend any more on energy (or momentum), so the Gaussian weights needed (for $-5 \leq n \leq +5$, say) can be computed once and for all before the calculation begins. Another bonus of Turing's method is the introduction of a natural grid depending only on the effective temperature, which is convenient for fast point cross section calculation, producing automatically less points at higher temperatures where broadened cross sections are smoother. The method is convenient not only for cross section fitting, as is sometimes thought, but quite generally whenever Doppler-broadened multi-level point cross sections are needed. The program DOBRO is written along these lines (Fröhner 1980). Employing the exact free-gas kernel it generates Doppler-broadened MLBW and Reich-Moore cross sections about equally fast as SLBW cross sections from given resonance parameters. The trick is not to insist on Voigt profiles but to apply the usual technique for their computation - Turing's method - directly to the multi-level cross section expressions.

2.5.5 Broadening of Tabulated, Linearly Interpolable Point Data

A widely used method for the generation of Doppler-broadened resonance cross sections starts from natural cross sections σ_k given at energies E_k such that for any intermediate energy E linear interpolation is possible,

$$\sigma(E) = \frac{(E - E_k)\sigma_{k+1} + (E_{k+1} - E)\sigma_k}{E_{k+1} - E_k} \qquad (E_k \leq E \leq E_{k+1}) \tag{123}$$

with some specified accuracy. The linear variation with energy translates into a quadratic variation with speed,

$$\sigma(v) = a_k + b_k v^2 , \tag{124}$$

where a_k and b_k are constant coefficients. Such linearly interpolable point cross section tables are given in many evaluated nuclear data files. Insertion in (112) yields

$$\bar{\sigma}(v) = \sum_k \int_{w_k}^{w_{k+1}} \frac{dw}{u_T} \frac{w^2}{v^2} \left[e^{-(w-v)^2/u_T^2} - e^{-(w+v)^2/u_T^2} \right] (a_k + b_k w^2) . \tag{125}$$

Each sum term corresponds to a linear piece of the cross section representation. Substituting $x = (w - v)/u_T$ we find that for each sum term we need the integrals

$$\frac{2}{\sqrt{\pi}} \int_{x_k}^{x_{k+1}} dt\, e^{-t^2} t^n = I_n(x_k) - I_n(x_{k+1}) \qquad \text{for} \qquad n = 0, 1, 2, 3, 4 \tag{126}$$

with

$$I_n(x) \equiv \frac{2}{\sqrt{\pi}} \int_x^\infty dt\, e^{-t^2} t^n = \frac{1}{\sqrt{\pi}} e^{-x^2} x^{n-1} + \frac{n-1}{2} I_{n-2}(x) . \tag{127}$$

I_0 and I_1 are easily calculated whereupon the others can be obtained with the last recursion relation (that results from partial integration):

$$
\begin{aligned}
I_0(x) &= \operatorname{erfc} x \,, \\
I_1(x) &= \frac{1}{\sqrt{\pi}} \,, \\
I_2(x) &= \frac{1}{2} \operatorname{erfc} x + \frac{1}{\sqrt{\pi}} e^{-x^2} x \\
I_3(x) &= \frac{1}{\sqrt{\pi}} e^{-x^2} (x^2 + 1) \,, \\
I_4(x) &= \frac{3}{4} \operatorname{erfc} x + \frac{1}{\sqrt{\pi}} e^{-x^2} (x^3 + \frac{3}{4} x) \,,
\end{aligned} \tag{128}
$$

This is the basis of the SIGMA1 code (Cullen and Weisbin 1976). It should be noted that in spite of the title of the paper the method is not exact since the linear interpolation between the tabulated cross sections is an approximation that introduces some error. (In modern evaluated files relative errors up to 1 % or at best 0.5 % are admitted for each linear piece.) It should also be realised that exponentials and error functions must be calculated for each linear piece of the cross section representation. If the cross sections σ_k are not given but must be calculated first, the SIGMA method is definitely slower and in any case less accurate than the Turing approach, and the choice of an irregular grid permitting interpolation with a specified accuracy, with a minimum of grid points, may be problematic, whereas the Turing method provides a suitable grid automatically.

2.5.6 Westcott Factors

The energy spectrum of neutrons in a thermal reactor can be roughly described by the Maxwellian energy distribution that follows from (107) upon integration over angles,

$$
p(E)dE = \frac{2}{\sqrt{\pi}} \exp\left(-\frac{E}{kT}\right) \sqrt{\frac{E}{kT}} \frac{dE}{kT} \,, \tag{129}
$$

plus a $1/E$ tail towards high energies. The (n,x) reaction rate induced by such a spectrum is given in good approximation by

$$
\int_0^\infty dE\, p(E) \sqrt{E}\, \bar{\sigma}_x(E) \equiv \sqrt{kT}\, \sigma_x(kT)\, g_W \,, \tag{130}
$$

where $\bar{\sigma}_x(E)$ under the integral is the (n,x) cross section Doppler broadened to the temperature T, $\sqrt{kT}\,\sigma_x(kT)$ is the result one would get for a $1/v$ cross section, and the Westcott factor g_W corrects this reaction rate for the actual deviations from a $1/v$ shape. Westcott factors for the thermal energy $kT = 25.3$ meV, corresponding to $v = 2200$ m/s, are convenient for reaction rate calculations in thermal fluxes since thermal (2200 m/s) cross sections are well known (see e. g. the barn book, Mughabghab et al. 1981, 1984) and since low-energy reaction cross sections usually exhibit $1/v$ shapes modified only slightly by the tails of nearby levels, including the invisible ("negative", bound) levels just below the neutron reaction threshold.

3. The Statistical Model of Resonance Reactions

With statistical distributions of level spacings and partial widths, scaled by given averages of these quantities, one can calculate average cross sections and cross section fluctuations in the unresolved resonance region, and more general functionals of the cross sections such as group constants for reactor safety and shielding studies. The statistical model of resonance reactions emerged in the 'fifties (see Porter 1965 for key publications) but important results are quite recent, for instance the solution of the so-called Hauser-Feshbach problem discussed below.

3.1 Resonance Statistics

We shall begin with an overview of basic level statistics, in particular the (local) distributions of the R-matrix resonance parameters, viz. level energies E_λ and decay amplitudes $\gamma_{\lambda c}$.

3.1.1 The Porter-Thomas Hypothesis

We have seen (Sect. 2.3, Eq. 46) that the decay amplitudes $\gamma_{\lambda c}$ of R-matrix theory are essentially values of the internal radial eigenfunctions at the channel entrance. Generally they represent the overlap of the λ-th eigenfunction and the external (channel) wave function at $r_c = a_c$. For a compound system with $A+1$ nucleons they are $(3A+2)$-dimensional integrals over the surface of the internal region in configuration space. The integrands oscillate rapidly so that positive and negative contributions largely cancel. The integrals are therefore nearly zero, and positive or negative with equal probability, depending on the unknown particulars of the λ-th eigenstate. Under these circumstances a Gaussian distribution of the $\gamma_{\lambda c}$ with mean zero seems to be a reasonable guess. In fact, the maximum entropy principle of probability theory (see Jaynes 1983, also Fröhner 1990) tells us that, if we know only that the distribution has zero mean and finite spread (variance), our most objective choice is indeed the Gaussian,

$$p(\gamma_c)d\gamma_c = \frac{1}{\sqrt{\pi}} e^{-x^2}\, dx\,, \qquad -\infty < x \equiv \frac{\gamma_c}{\sqrt{2\langle\gamma^2\rangle}} < \infty\,. \tag{131}$$

With $d\gamma_c^2 = 2\gamma_c d\gamma_c$ and $p(\gamma_c)d\gamma_c \equiv p(\gamma_c^2)d\gamma_c^2$ this becomes the distribution proposed by Porter and Thomas (1956),

$$p(\gamma_c^2)d\gamma_c^2 = \frac{e^{-y}}{\sqrt{\pi y}} dy \qquad 0 < y \equiv \frac{\gamma_c^2}{2\langle\gamma_c^2\rangle} < \infty\,, \tag{132}$$

for partial widths $\Gamma_{\lambda c} = 2P_c\gamma_{\lambda c}^2$ for single channels (and at a given energy). Examples for single-channel widths are reduced neutron widths for $I = 0$ or $\ell = 0$ (see Table 1) or partial radiation widths for single radiative transitions, not only in nuclear but also in atomic and molecular spectroscopy. The single-channel Porter-Thomas distribution agrees well with observed distributions of single-channel reduced neutron widths and single-transition photon widths. Note that the smallest widths are the most frequent ones.

Many observable widths are, however, sums of single-channel widths, for instance neutron widths for $I > 0$ or $\ell > 0$, or total radiation widths, or fission widths. If the averages

$\langle\gamma_c^2\rangle$ were the same for all ν contributing channels, such an observable width would obey the generalised Porter-Thomas distribution, i. e. a χ^2-distribution with ν degrees of freedom,

$$p(\gamma_x^2)d\gamma_x^2 = \Gamma(\nu/2)^{-1}e^{-y}y^{\nu/2-1}dy\,, \qquad 0 < y \equiv \frac{\nu\gamma_x^2}{2\langle\gamma_x^2\rangle} < \infty\,, \tag{133}$$

where $\Gamma(\nu/2)$ is the Gamma function, and

$$\gamma_x^2 \equiv \sum_{c\in x}\gamma_c^2\,, \tag{134}$$

$$\langle\gamma_x^2\rangle = \nu\langle\gamma_c^2\rangle\,. \tag{135}$$

The generalised Porter-Thomas distribution applies to two-channel reduced neutron widths ($\nu = 2$, exponential distribution) and, with an effective (not necessarily integer) number ν of fission channels, to fission widths (ν small) and to total radiation widths (ν large, delta-like distribution: radiation widths fluctuate little from level to level). Large effective ν for total radiation widths are not unexpected because of the usually large number of allowed radiative transitions to lower-lying compound states. That ν is small for total fission widths, however, was a surprise. The hundreds of possible pairs of fission fragments, each with many possible excited states, would seem to imply equally many partial fission widths, and a correspondingly large effective ν.

The puzzle was solved by A. Bohr (1955). He pointed out that before scission can occur the compound system must pass the saddle point of the potential-energy surface (in the space of deformation parameters) beyond which Coulomb repulsion prevails over nuclear cohesion. At the saddle point most of the energy released in fission is tied up as deformation energy, so only little remains for other modes of excitation whose spectrum resembles that of the low-lying states observed at the ground state deformation. Energy, angular momentum and parity conservation allow access to only few of these transition states, regardless of the huge number of final partitions. Therefore the fission channels are correlated in such a way that the fission width can be approximated as a sum over a small number of terms, one for each transition state ("saddle point channel"). For fission, therefore, ν is the effective number of open saddle point channels rather than the number of reaction channels in the usual sense.

This illustrates that the level-statistical "laws" are not nearly as rigid as the resonance formalism discussed in Section 2. They hold mainly for highly excited compound states for which all single-particle, collective or other simplicity is lost. Reflecting more our ignorance than truly random phenomena they may be inapplicable if the states considered are simple and well understood. Recognition of the role of collective transition states of a fissioning nucleus enabled us to modify and, in fact, to simplify the statistical description of fission resonances. In our single-particle exercise with a complex square-well potential nothing at all was random or unspecified, and the reduced neutron widths turned out to be all the same instead of exhibiting a Porter-Thomas distribution, see Eq. 60.

3.1.2 Wigner's Surmise and the Gaussian Orthogonal Ensemble

It turned out to be much more difficult to find the distribution of level spacings in a given $J\Pi$ level sequence than to find the partial-width distributions. Early in the game Wigner (1957) tried a bold guess. He took issue with the Poisson distribution tried by others

according to which the probability of finding a level spacing $E_{\lambda+1} - E_\lambda$ in a small interval dD at D is just proportional to dD, independent of the distance to the preceding level. He pointed out that level energies are eigenvalues of Hamilton matrices, and that these matrices always exhibit eigenvalue repulsion (vanishing probability for zero level spacing) so that at least for small spacings the probability should be proportional to DdD. Assuming proportionality also for large D he got immediately what is now known as Wigner's surmise,

$$p(D)dD = \exp(-c\int_0^D D'dD')cDdD = ce^{-cD^2/2}DdD\,. \tag{136}$$

In terms of the mean level spacing the proportionality constant is $c = \pi/(2\langle D\rangle^2)$.

The theory of Hamiltonian matrix ensembles (that is, of probability distributions for Hamilton matrices) was subsequently developped by Wigner, Porter, Dyson, Mehta and others (see Porter 1965, Brody et al. 1981). Nuclear Hamiltonian matrices are Hermitean, of course, but also, due to the practical invariance of nuclear interactions under time reversal, symmetric and thus real. If we knew a probability distribution of such matrices we could derive the corresponding distribution of eigenvalues. The simplest ensemble is obtained if we assume nothing but a finite spread of the eigenvalue spectrum, which is well supported by the Gaussian-like eigenvalue distributions resulting from shell model calculations (see Brody et al. 1981). Maximising the entropy of the distribution under the constraint of finite spread (see e. g. Fröhner 1990, 1991a) one finds as the most objective choice

$$p(\mathbf{H})d(\mathbf{H}) \propto \prod_\mu \exp\left(-\lambda H_{\mu\mu}^2\right)dH_{\mu\mu} \prod_{\mu<\nu} \exp\left(-2\lambda H_{\mu\nu}^2\right)dH_{\mu\nu}\,, \quad \lambda = \frac{N+1}{2\sigma^2} \tag{137}$$

where N is the rank of the matrix $\mathbf{H}$ (the number of eigenvalues), $d(\mathbf{H})$ the volume element in the space of independent matrix elements, and σ the spread of the eigenvalue spectrum (around its centre at E = 0). Having maximal entropy (minimal information content) among all distributions of real, symmetric matrices with given dispersion σ, our ensemble plays a similar role for those matrices as a Gaussian distribution does for scalar distributions with given spread. It is called the Gaussian orthogonal ensemble (GOE) because it is invariant under orthogonal transformations and because the matrix elements have independent Gaussian distributions. Actually Wigner derived it from the requirements of rotational invariance (all orthogonal bases must be equivalent in quantum mechanics) and of independently distributed matrix elements, but the independence requirement was criticised as unphysical, in seeming conflict with the predominant two-body character of nuclear forces. In the maximum entropy approach independence is a natural consequence of the limited input information. In any case Wigner's suggestion that the GOE provides a mathematically simple model of level statistics has been fully confirmed. Porter and Rosenzweig (1960) demonstrated that for very large matrices (very many compound states) the GOE yields the Porter-Thomas distribution of partial widths. The level spacing distribution for 2×2 matrices is exactly Wigner's surmise, while for larger matrices it is very close as shown by Mehta (1960) and Gaudin (1961), see Fig. 9.

The level spacings are correlated in such a way that a relatively large spacing is followed by a short one more often than not, and vice versa. The resulting correlation coefficient is

$$\rho(D_\lambda, D_{\lambda+1}) \equiv \frac{\mathrm{cov}\,(D_\lambda, D_{\lambda+1})}{\sqrt{\mathrm{var}\,(D_\lambda)\,\mathrm{var}\,(D_{\lambda+1})}} \simeq -0.27 \tag{138}$$

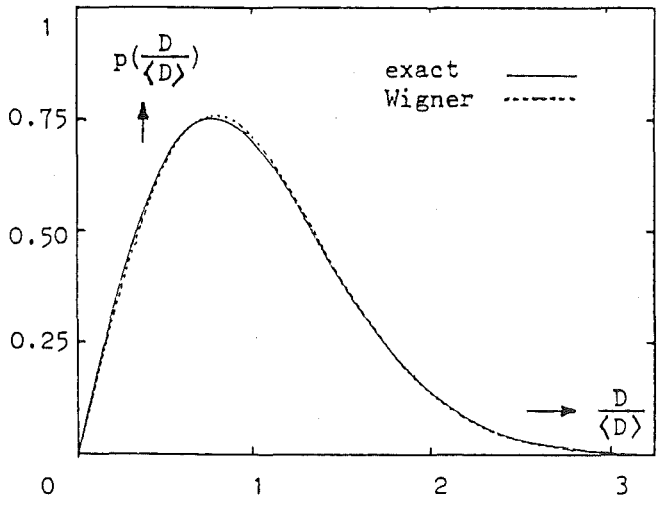

Fig. 9. Next-nearest neighbour spacing distribution for the Gaussian Orthogonal Ensemble of real, symmetric matrices. Solid line: large $N \times N$ matrices, limit $N \to \infty$ (Gaudin 1961). Dotted line: 2×2 matrices (Wigner distribution, Eq. 132)

for large matrices. The eigenvalue sequence has thus a remarkable regularity, the spectrum is "stiff". All this is in excellent agreement with observed nuclear (and atomic) level statistics, at least in limited energy ranges where variations of the level density and average partial widths can be neglected. Seeming deviations from GOE predictions usually vanish if the long-range ("secular") variations of the average parameters are properly taken into account.

3.1.3 Secular Variations of Level Statistics

The Gaussian orthogonal ensemble, constrained only by the finite spread of the eigenvalue spectrum, cannot be expected to reproduce model-dependent global features such as Fermi-gas level densities, shell effects, giant dipole resonances or fission barrier effects. In fact, the semi-circular GOE level density obtained by Wigner (1957) differs from the Gaussian-like densities found in more realistic shell model calculations (see Brody et al. 1981). Although the distributions of level energies and partial widths can locally be taken as those of the GOE, their parameters (level density, average widths) vary slowly with energy. These secular variations are described by macroscopic models of the nucleus - level densities, for instance, by the Fermi-gas model or, at higher energies, by the shell model with residual interaction; neutron, proton and alpha particle strength functions by the optical model; photon strength functions by the giant-dipole resonance model; fission strength functions by fission barrier models. These models are discussed by others in the present volume, so we shall not go into any detail here but concentrate on the calculation of average cross sections and cross section functionals. The theory of resonance-averaged cross sections, Hauser-Feshbach theory, provides statistical (GOE) averages over R-matrix cross

section expressions. The essential input for these calculations are so-called transmission coefficients,

$$T_c \equiv 1 - |\bar{U}_{cc}|^2 = \frac{4\pi s_c P_c}{|1 - \bar{R}_{cc} L_c^o|^2}\,, \tag{139}$$

with $\bar{R}_{cc} \equiv R_c^\infty + i\pi s_c$. This is essentially 2π times the ratio of average effective neutron width to mean level spacing (compare Eqs. 70 and 108). For photon and fission channels one uses accordingly

$$T_\gamma = 2\pi \frac{\bar{\Gamma}_\gamma}{D_c}\,, \tag{140}$$

$$T_f = 2\pi \frac{\bar{\Gamma}_f}{D_c}\,. \tag{141}$$

The mean level spacing $D_c = 1/\rho_J$ plays the role of a scale factor. Its J dependence is given by

$$\begin{aligned} \rho_J &\propto \exp\Big[-\frac{J^2}{2\sigma^2}\Big] - \exp\Big[-\frac{(J+1)^2}{2\sigma^2}\Big] \\ &\propto \sinh\Big(\frac{J+1/2}{2\sigma^2}\Big) \exp\Big[-\frac{(J+1/2)^2}{2\sigma^2}\Big] \end{aligned} \tag{142}$$

(Bethe 1937, Gilbert and Cameron 1965) where the dispersion σ is called the spin cut-off. For $J \ll \sigma$ one gets $\rho_J \propto 2J+1$ which is accurate enough for many purposes.

4.2 Resonance-averaged Cross Sections

A typical problem in the unresolved resonance region is that average cross sections or cross section functionals like the average transmission are to be calculated, in an averaging interval wide enough to contain many resonances but so narrow that variations of level statistics and other weak energy dependences can be neglected. We may then simplify our equations by choosing boundary parameters such that locally $L_c^o = iP_c$, and by absorbing P_c in the decay widths $\gamma_{\lambda c}$. Furthermore, we shall write $\mathbf{S}$ instead of $\mathbf{U}$ for the S matrix, as is customary in the literature on average cross sections. The average collision matrix is then (compare Eqs. 17-22, 51-55)

$$\begin{aligned} \bar{S}_{ab} &= e^{-i(\varphi_a + \varphi_b)} \big[(\mathbf{1} - i\bar{\mathbf{R}})^{-1}(\mathbf{1} + i\bar{\mathbf{R}})\big]_{ab} \\ &= e^{-i(\varphi_a + \varphi_b)} \Big(\delta_{ab} + 2i\overline{\sum_{\lambda,\mu} \gamma_{\lambda a} A_{\lambda\mu} \gamma_{\lambda b}}\Big)\,, \end{aligned} \tag{143}$$

with

$$(\mathbf{A}^{-1})_{\lambda\mu} = (E_\lambda - E)\delta_{\lambda\mu} - i\sum_c \gamma_{\lambda c}\gamma_{\mu c}\,. \tag{144}$$

3.2.1 Average Total Cross Section

In order to average the total cross section we must average the collision matrix element S_{cc} over energies. This is easy if we use a Lorentzian weight function,

$$\begin{aligned} \bar{\mathbf{S}}(E) &= \int_{-\infty}^{\infty} dE' \, \frac{I/\pi}{(E'-E)^2 + I^2}\, \mathbf{S}(E') \\ &= \frac{1}{2\pi i} \int_{-\infty}^{\infty} dE' \Big(\frac{1}{E' - E - iI} - \frac{1}{E' - E + iI}\Big) \mathbf{S}(E')\,, \end{aligned} \tag{145}$$

where $2I$ is the full width at half maximum of the Lorentzian. Because of causality S has no poles above the real axis (see Lane and Thomas 1958), so if we close the contour by a large upper semicircle it encloses only one pole of the Lorentzian, $E+iI$, and the residue is

$$\bar{\mathrm{S}}(E) = \mathrm{S}(E+iI)\,. \tag{146}$$

As we neglect weak energy dependences we need only replace $\mathbf{R}(E)$ by $\mathbf{R}(E+iI)$, with

$$\begin{aligned} R_{ab}(E+iI) &= \sum_{\lambda} \frac{\gamma_{\lambda a}\gamma_{\lambda b}}{E_\lambda - E - iI} \\ &\simeq \int_{-\infty}^{\infty} \frac{dE'}{D_c}\,\frac{\gamma_a\gamma_b}{E'-E-iI} \simeq \int_{-\infty}^{\infty} dE'\,\frac{s_a(E')}{E'-E-iI}\delta_{ab}\,. \end{aligned} \tag{147}$$

In the last approximation we exploited the fact that because of the random signs of the $\gamma_{\lambda c}$ the average matrix $\overline{\gamma_{\lambda a}\gamma_{\lambda b}}$ is practically diagonal, and we used the definition of the pole strength, Eq. 54. If finally we consider I as a small quantity, and write $\bar{\mathbf{R}}$ instead of $\mathbf{R}(E+iI)$, we get

$$\bar{R}_{cc} = R_c^{\infty} + i\pi s_c, \tag{148}$$

$$\bar{S}_{cc} = 2\pi\lambda\!\!\!^{-2}_c g_c\left[1 - \mathrm{Re}\left(e^{-2i\varphi_c}\frac{1+i\bar{R}_{cc}}{1-i\bar{R}_{cc}}\right)\right]. \tag{149}$$

The average total cross seciton is thus expressed by the pole strength and the distant-level parameter, quantities that can be obtained either by statistical analysis of resolved resonances or from optical-model calculations (for given channel radius).

3.2.2 Partial Cross Sections: Heuristic Recipes

The average partial cross section,

$$\bar{\sigma}_{ab} = \pi\lambda\!\!\!^{-2}_a g_a \overline{|\delta_{ab} - S_{ab}|^2}\,, \tag{150}$$

is no linear function of S but requires averaging over quadratic terms like $S^*_{ab}S_{cd}$. These have poles above as well as below the real axis which prevents contour integration with a Lorentzian weight function. Under the usual ergodicity and stationarity conditions of good statistics - many resonances and negligible variation of the parameter distributions within the averaging interval - one can replace the energy average by an ensemble average (expectation value) over the GOE, i. e. over the joint distribution of level energies and decay amplitudes. The ensemble average is readily obtained in the limit of widely spaced ("isolated") resonances that overlap so weakly that multi-level effects and eigenvalue correlations can be neglected. Assuming generalised Porter-Thomas (χ^2) distributions for the partial widths one obtains in many-level SLBW approximation

$$\sigma_{ab} = \sigma_{p,a}\delta_{ab} + \pi\lambda\!\!\!^{-2}_a g_a \frac{T_a T_b}{T}\left(1 + \frac{2}{\nu_a}\delta_{ab}\right)\int_0^{\infty} dx \prod_c \left(1 + \frac{2T_c}{\nu_c T}x\right)^{-\delta_{ac}-\delta_{bc}-\nu_c/2} \tag{151}$$

(Dresner 1957, Lane and Lynn 1957), where $\sigma_{p,a}$ is the potential-scattering cross section, $T_c \equiv 1 - |\bar{S}_{cc}|^2$ is the transmission coefficient for channel c, $T \equiv \sum_c T_c$, and ν_c the degree

of freedom for the partial widths $\Gamma_{\lambda c} = 2\gamma_{\lambda c}^2$ (remember that P_c is absorbed in $\gamma_{\lambda c}^2$). The approximation $T_c \simeq 2\pi\bar{\Gamma}_c/D_c$, valid for vanishing level overlap, was used to write the result in terms of the T_c. This is the Hauser-Feshbach formula with elastic enhancement (first pair of parentheses) and width fluctuation correction (integral) - see Moldauer (1975). We recall that $\nu_c = 1$ for single channels but that in practical applications one often uses lumped channels, with an effective $\bar{\nu}_c$ differing from unity, in order to represent e. g. all fission or capture channels or all particle channels that have the same total angular momentum and parity and thus involve the same compound levels. The number of photon channels is usually so large (except for light and magic nuclei) that one may put

$$\prod_{c\in\gamma}\left(1+\frac{2T_c}{\nu_c T}x\right)^{-\bar{\nu}_c/2} \simeq \lim_{\bar{\nu}_\gamma\to\infty}\left(1+\frac{2T_\gamma}{\bar{\nu}_\gamma T}x\right)^{-\bar{\nu}_\gamma/2} = e^{-xT_\gamma/T}\,. \tag{152}$$

So the many photon channels can be simply represented by an exponential.

Generalisation of the Hauser-Feshbach formula to arbitrary level overlap turned out to be extremely difficult. Of course one could always resort to Monte Carlo sampling of level spacings and decay amplitude from their probability distributions, with subsequent point cross section calculation and averaging. The desired cross section average is thus obtained, although with the statistical uncertainty and lack of transparency typical for the Monte Carlo method. From such numerical Monte Carlo studies two practically important recipes were deduced heuristically, by trial and error and educated guesswork.

The first recipe, due to Moldauer (1980), consists in using the Hauser-Feshbach formula, strictly valid only for weak level overlap, also for strong overlap, but with $\sigma_{p,a}$ interpreted as the "direct" cross section,

$$\sigma_{p,a} = \pi\lambda\!\!\!^{-2}_a g_a |1-\bar{S}_{aa}|^2\,, \tag{153}$$

and with the exact expression for the particle-channel transmission coefficients,

$$T_a = \frac{4\pi s_a}{|1-i\bar{R}_{aa}|^2}\,. \tag{154}$$

Furthermore, the ν_c are considered as depending on the T_c. The dependence is chosen so as to fit a large body of Monte Carlo results while giving the correct limit for small level overlap (for small transmission coefficients). Moldauer's heuristic recommendation is

$$\bar{\nu}_c = [1.78 + (T_c^{1.218} - 0.78)e^{-0.228\,T}]\nu_c\,. \tag{155}$$

The second practically important prescription is due to Hofmann, Richert, Tepel and Weidenmüller (1975) who, in the spirit of Bohr's original compound-nuclear model (with no memory of compound formation), take the partial cross sections as factorisable,

$$\bar{\sigma}_{ab} = \sigma_{p,a}\delta_{ab} + \pi\lambda\!\!\!^{-2}_a g_a \frac{V_a V_b}{V}\left[1+(\omega_a-1)\delta_{ab}\right]\,, \tag{156}$$

with $V \equiv \sum_c V_c$. The elastic enhancement factors ω_c are expected to approach 3 for vanishing and 2 for very strong level overlap (Satchler 1963). The authors found their Monte Carlo results adequately reproduced with

$$\omega_a = 1 + \frac{2}{1+T_a^{0.3+1.5\,T_a/T}} + 2\left(\frac{T_a}{T}-\frac{1}{n}\right)^2\,, \tag{157}$$

where n is the number of open channels. With these heuristic values of the ω_a one can calculate the V_a from

$$V_a = \frac{T_a}{1 + (\omega_a - 1)V_a/V} \,. \tag{158}$$

by iteration, beginning with $V_c = T_c$. The last equation follows from the unitarity of S.

Both prescriptions yield similar results for intermediate and strong absorption (medium and strong level overlap). Moldauer's recipe is convenient for lumped channels and, by construction, it yields the correct limit for vanishing overlap and few (nonphotonic) channels at low energies where the factorisation approximation fails. Other approximate analytic expressions were derived with picket fence models (e. g. Janeva et al. 1985) and disordered picket fence models (Müller and Harney 1987).

3.2.3 Maximum-Entropy Distributions of the R and S Matrix

For decades all attempts to average the partial cross ssection expressions rigorously failed. In this situation information theory seemed to offer a possibility to bypass all "microscopic" resonance details completely by treating them as a kind of noise superimposed on the "macroscopic" average behaviour described for instance by the optical model. This approach was pioneered by Mello (1979) who invoked the maximum entropy principle (see Jaynes 1983) which states that for a given average (e. g. optical-model) S matrix the most objective S matrix distribution to be used for predictions is the one with the highest entropy (least information) and with just the given average. Mello, Pereyra and Seligman (1985) found that the so-called Poisson kernel defined in the domain of unitary symmetric matrices (Hua 1963),

$$p(\mathbf{S}|\bar{\mathbf{S}})d(\mathbf{S}) \propto \left(\frac{\det \mathbf{T}}{\det |\mathbf{1} - \bar{\mathbf{S}}^\dagger \mathbf{S}|^2}\right)^{(n+1)/2} d(\mathbf{S}) \,, \tag{159}$$

seems to be the required distribution, having all the properties demanded by ergodicity and by the analytic structure of the S matrix, while its form implies maximal entropy given the average S matrix $\mathbf{S}$. (Our notation here is the usual one for conditional probabilities, $d(\mathbf{S})$ is the volume element in the space of independent real and imaginary parts of the S-matrix elements, $\mathbf{T} \equiv \mathbf{1} - \bar{\mathbf{S}}^\dagger \bar{\mathbf{S}}$ is the transmission matrix generalising the usual definition of transmission coefficients, and n is the rank of $\mathbf{S}$, i. e. the number of open channels.)

The same result was found independently by Fröhner (1986), who derived the maximum entropy distribution of R matrices for given $\bar{R}_{ab} = (R_a^\infty + i\pi s_a)\delta_{ab}$,

$$p(\mathbf{R}|\bar{\mathbf{R}})d(\mathbf{R}) \propto \frac{\prod_{a \le b} dX_{ab}}{\det (\mathbf{1} + \mathbf{X}^2)^{(n+1)/2}} \,, \qquad -\infty < X_{ab} \equiv \frac{R_{ab} - R_a^\infty \delta_{ab}}{\pi\sqrt{s_a s_b}} < \infty \,, \tag{160}$$

which is a matrix generalisation of Student's t distribution familiar from statistics. Rewriting it in terms of S one finds the Poisson kernel (for details see Fröhner 1990). Eq. 160 looks less compact than Eq. 159, but in fact it is more practical and its derivation is more straightforward because dealing with real symmetric matrices is much easier than dealing with unitary symmetric ones. In fact the volume element $d(\mathbf{S})$ must be expressed in terms of $\mathbf{R}$ before it becomes practically useful at all, and in the literature there has been some confusion about it ("Dyson's measure").

In principle one could calculate average cross sections as ensemble averages

$$\bar{\sigma}_{ab} = \int \sigma_{ab}\, p(\mathbf{R}|\bar{\mathbf{R}}) d(\mathbf{R}) = \int \sigma_{ab}\, p(\mathbf{S}|\bar{\mathbf{S}}) d(\mathbf{S}). \tag{161}$$

The dimensionality of these integrals is $n(n+1)/2$ for n open channels. Introducing "polar" coordinates, i. e. the eigenvalues and the angles of the rotation leading to the principal-axes system, one can integrate over all possible rotations and reduce the dimensionality to n.

In general, however, first experience with the Poisson kernel or the generalised t distribution shows that their compact determinantal structure makes them rather intractable. It seems difficult to find practical ways to use them, i. e. to find suitable expansions, to reduce the dimensionality of the integrals, to verify that the Hauser-Feshbach formula with width fluctuations is obtained in the limit of vanishing level overlap, and to deal with the many weakly absorbing photon channels in a similar way as in Eq. 152. Before any progress in this direction could be achieved there was success on the microscopic level.

3.2.4 The GOE Triple Integral.

Only a few months after the maximum-entropy distributions of the S and R matrix had been published Verbaarschot, Weidenmüller and Zirnbauer (1985) presented an analytic solution to the long-standing Hauser-Feshbach problem of finding an analytic expression for the average partial cross sections, i. e. to average analytically over the GOE resonance parameter distributions given the transmission coefficients (average partial widths scaled by the mean level spacing). These authors started from an expression involving a GOE Hamiltonian coupled to the channels. In our notation it reads

$$|S_{ab}|^2 = |\delta_{ab} + i \sum_{\lambda,\mu} \tilde{\gamma}_{\lambda a} A_{\lambda\mu} \tilde{\gamma}_{\mu b}|^2 \,, \tag{162}$$

$$(\mathbf{A}^{-1})_{\lambda\mu} = H_{\lambda\mu} - E\delta_{\lambda\mu} - i \sum_{c} \tilde{\gamma}_{\lambda c} \tilde{\gamma}_{\mu c} \,, \tag{163}$$

which is a generalisation of what Eqs. 20-22 give for $|S_{ab}|^2$: The tilde indicates that the Hamiltonian is taken in its nondiagonal form, so that $H_{\lambda\mu}$ and $\tilde{\gamma}_{\lambda a}$ replace $E_\lambda \delta_{\lambda\mu}$ and $\gamma_{\lambda a}$ of Eq. 22. By a formidable display of analytic skill the authors managed, with new tools from the many-body theory of disordered systems, to reduce the ensemble average (expectation value) of $|S_{ab}|^2$ over the GOE to a threefold integral. Making full use of the symmetries of the GOE, of a generating function involving both commuting and anticommuting (Grassmann) variables, of the Hubbard-Stratonovitch transformation to simplify the integrations, then going to the limit of infinitely many levels ($n \to \infty$ for the rank of H) by the method of steepest descent, they derived the awsome expression

$$\begin{aligned}
\overline{|S_{ab}|^2} = |\bar{S}_{ab}|^2 + \frac{T_a T_b}{8} \int_0^\infty d\lambda_1 \int_0^\infty d\lambda_2 \int_0^1 d\lambda \frac{\lambda(1-\lambda)|\lambda_1 - \lambda_2|}{\sqrt{\lambda_1(1+\lambda_1)}\sqrt{\lambda_2(1+\lambda_2)}(\lambda+\lambda_1)^2(\lambda+\lambda_2)^2} \\
\times \left(\prod_c \frac{1 - T_c\lambda}{\sqrt{1+T_c\lambda_1}\sqrt{1+T_c\lambda_2}} \right) \left\{ \delta_{ab}(1-T_a) \left(\frac{\lambda_1}{1+T_a\lambda_1} + \frac{\lambda_2}{1+T_a\lambda_2} + \frac{2\lambda}{1-T_a\lambda} \right)^2 \right. \\
\left. + (1+\delta_{ab}) \left(\frac{\lambda_1(1+\lambda_1)}{(1+T_a\lambda_1)(1+T_b\lambda_1)} + \frac{\lambda_2(1+\lambda_2)}{(1+T_a\lambda_2)(1+T_b\lambda_2)} + \frac{2\lambda(1-\lambda)}{(1-T_a\lambda)(1-T_b\lambda)} \right) \right\}
\end{aligned} \tag{164}$$

for the absolute square of the collision matrix element that had caused the difficulties with its poles below and above the real axis in the complex energy plane. We have here a three-dimensional integral no matter how many open reaction channels there are. Furthermore, the channel product allows a similar treatment of the many weakly absorbing photon channels as in the Hauser-Feshbach formula:

$$\prod_c \frac{1-T_c\lambda}{\sqrt{1+T_c\lambda_1}\sqrt{1+T_c\lambda_2}} \approx e^{-(\lambda_1+\lambda_2+2\lambda)T_\gamma/2} \prod_{c\notin\gamma} \frac{1-T_c\lambda}{\sqrt{1+T_c\lambda_1}\sqrt{1+T_c\lambda_2}}\,, \qquad (165)$$

with $T_\gamma \equiv \sum_{c\in\gamma} T_c$ as in Eq. 152.

Verbaarschot (1986) verified that in the limit of small level overlap the GOE triple integral (164) yields the Hauser-Feshbach formula (151) with elastic enhancement and width fluctuation correction. He also compared averages computed with the triple integral and averages over the Poisson kernel. In spite of the utterly different appearance of the multiple integrals in the two approaches he found the same numbers to 3 or 4 digits, i. e. agreement within the numerical accuracy of the two calculations. This constitutes striking evidence for the irrelevance of "microscopic" resonance details and raises the question whether an analogous superintegration over the S- or R-matrix ensemble could not yield a simple form also. In any case the GOE triple integral, including elastic enhancement and width fluctuation corrections, is a rigorous solution to the Hauser-Feshbach problem, eliminating all uncertainties associated with picket fence models or heuristic analytic formulae derived from Monte Carlo results. These uncertainties had always been bothersome since width fluctuation corrections are often quite substantial (see e. g. Lynn 1968, Gruppelaar and Reffo 1977). An important point is that above a few meV resonance-averaged cross sections are practically independent of temperature: Energy averaging involves essentially sums over peak areas, and since those are invariant under Doppler broadening (in Kapur-Peierls, Adler-Adler, MLBW and SLBW form we have $\int dE\,\psi_\lambda = \pi\Gamma_\lambda/2$ and $\int dE\,\chi_\lambda = 0$, irrespective of temperature, see Appendix), the same is true for average cross sections. Thus the GOE triple integral, derived for unbroadened resonances, can also be used to calculate averages over Doppler-broadened resonances.

So far we treated mainly pure compound-nuclear reactions, for which the average R and S matrices are diagonal. At higher energies (above 1 MeV, say) direct reactions become increasingly important, and the average S matrix resulting from coupled-channels calculations (with a deformed complex potential) acquires nonvanishing off-diagonal elements. Formally, however, one can transform the case with direct interaction to the pure compound case by means of a transformation given by Engelbrecht and Weidenmüller (1973). In this context we note that the Poisson kernel and the corresponding R-matrix distribution are valid for any given average S matrix, whether diagonal or not.

3.3 Examples for Calculation of Average Cross Sections and Other Cross Section Functionals

Figs. 10-13 show recent average total, capture and inelastic scattering cross section data for ^{238}U and theoretical curves fitted to all the data simultaneously. The fitting was done by least-squares adjustment of average resonance parameters, viz. of s-, p-, d- and f-wave neutron strength functions (which are essentially transmission coefficients for neutron channels) and of radiation widths scaled by the mean level spacing (transmission coefficients

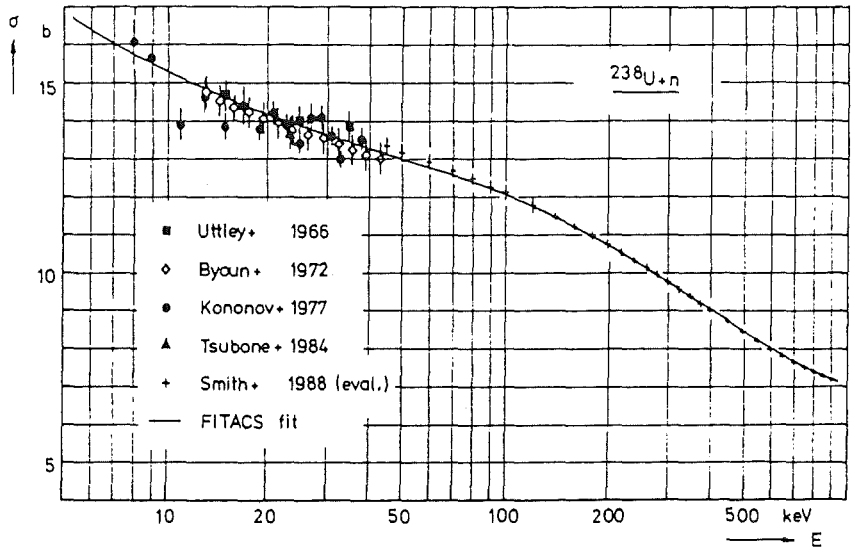

Fig. 10. Simultaneous Hauser-Feshbach fit to ^{238}U neutron data in the unresolved resonance region: total cross section (for references see Fröhner 1989)

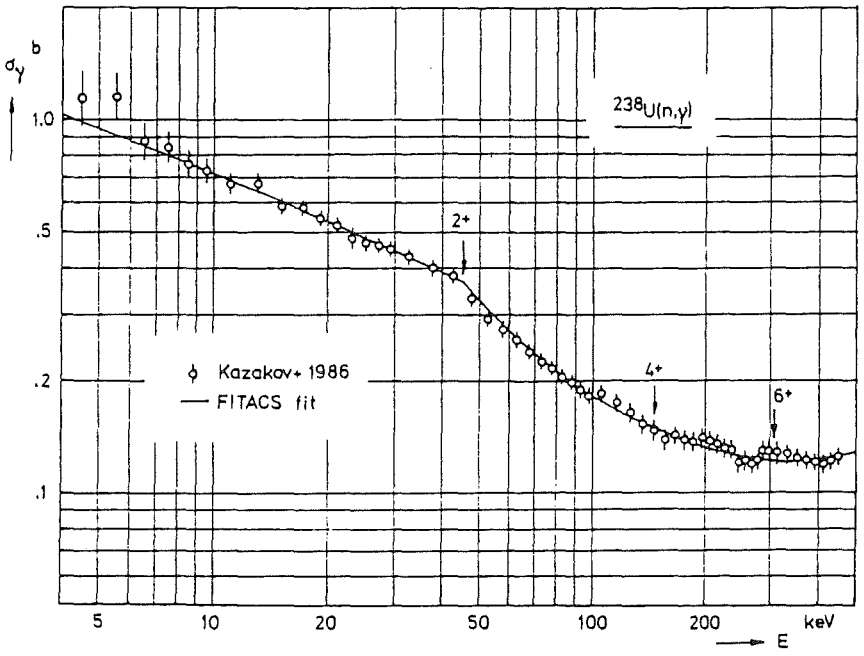

Fig. 11. Simultaneous Hauser-Feshbach fit to ^{238}U neutron data in the unresolved resonance region: capture cross section (for references see Fröhner 1989). The discontinuity (Wigner cusp) at 45 keV is due to competition by inelastic scattering above that energy. Inelastic thresholds are indicated by spin-parity characteristics of residual levels.

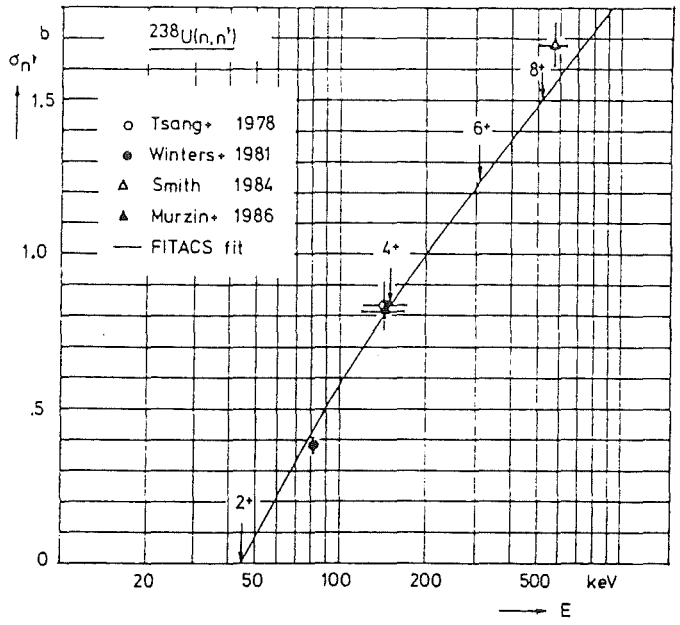

Fig. 12. Simultaneous Hauser-Feshbach fit to ^{238}U neutron data in the unresolved resonance region: inelastic-scattering cross section (for references see Fröhner 1989). Inelastic thresholds are indicated by spin-parity of residual levels.

for the lumped photon channels) with the code FITACS (Fröhner et al. 1982). The main energy dependences are introduced by the centrifugal-barrier penetration factors P_c for the neutron widths and by the employed composite level density formula of Gilbert and Cameron (1965), whereas the strength functions and radiation widths vary only little in the energy range covered. The total cross section was calculated with Eqs. 148-149, the partial cross sections with the Hauser-Feshbach formula in the form proposed by Moldauer (1980), Eqs. 151-155, and cross-checked with the GOE triple integral, Eqs. 164-165. Such fits to many more ^{238}U data defined eventually a new evaluation for ^{238}U in the unresolved resonance region that was adopted for the evaluated data libraries JEF-2 and ENDF/B-VI (Fröhner 1989). The final adjusted average resonance parameters are fully consistent with the resolved resonance parameters determined at lower energies, and also with optical-model calculations at higher energies up to 10 MeV. The error estimates from the least-squares fits indicate that, after decades of world-wide effort, the average total and capture cross sections of ^{238}U in the resolved resonance region are finally known with about the accuracies requested for applications in nuclear technology (1-3%). For inelastic scattering this goal is not yet achieved, the uncertainties there are still of the order of 5 - 15% .

Accurate average cross sections are, however, only part of the story. The other part concerns the resonance structure, i. e. the resonance fluctuations around the average cross section curves. They are implicitly given by the level-statistical model, in particular by the GOE distributions of level spacings and partial widths together with the mean values parametrising these distributions. The presence of unresolved resonance structure manifests

itself in sample-thickness and self-shielding effects. As the simplest illustration consider the relationship between the average transmission of a neutron filter, with thickness n (atoms/b) and an average total cross section $\bar{\sigma}$ of the shielding material,

$$\overline{e^{-n\sigma}} = e^{-n\bar{\sigma}}\,\overline{e^{-n(\sigma-\bar{\sigma})}} = e^{-n\bar{\sigma}}\left(1 + \frac{n^2}{2}\,\mathrm{var}\;\sigma - + \ldots\right) . \tag{166}$$

The last pair of parentheses represents a correction for resonance effects, containing the cross section variance (mean square fluctuation)

$$\mathrm{var}\;\sigma \equiv \overline{(\sigma - \bar{\sigma})^2} = \overline{\sigma^2} - \bar{\sigma}^2 \tag{167}$$

and higher moments of the cross section distribution which quantify the resonance structure. The correction is large for thick samples and strongly fluctuating cross sections, conditions which are encountered especially at the lower end of the unresolved resonance region. Thick-sample transmission measurements can therefore provide information about the resonance structure. If we want to compare experiments with calculations, however, we must average the transmission over resonances. In view of the experiences with GOE averaging of partial cross sections we must expect even worse problems for the average transmission. The need to deal with Doppler-broadened cross sections makes the problem patently hopeless as far as an analytic solution is concerned.

It is, however, perfectly straightforward to calculate such functionals of Doppler-broadened cross sections by Monte Carlo methods. An example is shown in Fig. 13, where thick-sample transmission data measured at room temperature are plotted together with Monte Carlo calculated curves. "Ladders" of resonances were defined by sampling resonance spacings from the Wigner distribution, Eq. 136, and of partial widths from Porter-Thomas distributions, Eq. 132, with average resonance parameters taken from the JEF-2 evaluation. The corresponding total cross section was calculated, Doppler broadened, exponentiated, and averaged. In this way 100 000 transmission values were sampled and averaged for each data point, so that the statistical error of the Monte Carlo results was negligible compared to the uncertainties of the data. The good agreement between experiment and calculation in Fig. 13 indicates that the JEF-2 evaluation describes not only the total cross section well (see Fig. 10) but also its resonance structure, e. g. the ratio of resonance (compound) to potential scattering (direct) cross sections, and the "windows".

More information about the cross section structure comes from self-indication measurements. Those differ from transmission measurements only insofar as the detector measuring the transmitted fraction of the neutron beam consists of a thin sample ("radiator"), made of the same material as the thick transmitting sample ("filter") and viewed by gamma ray detectors. From "filter in" and "filter out" runs one obtains the self-indication ratio

$$\frac{\overline{e^{-n\sigma}\sigma_\gamma}}{\bar{\sigma}_\gamma} = e^{-n\bar{\sigma}}\left(1 - n\frac{\mathrm{cov}\,(\sigma,\sigma_\gamma)}{\bar{\sigma}_\gamma} + - \ldots\right) \tag{168}$$

which involves the covariance between the total and capture cross section structure,

$$\mathrm{cov}\,(\sigma,\sigma_\gamma) \equiv \overline{(\sigma - \bar{\sigma})(\sigma_\gamma - \bar{\sigma}_\gamma)} = \overline{\sigma\sigma_\gamma} - \bar{\sigma}\bar{\sigma}_\gamma . \tag{169}$$

(For positive covariance the two arguments tend to vary in the same sense - if one increases, the other one is likely to increase too - for negative covariance they tend to vary

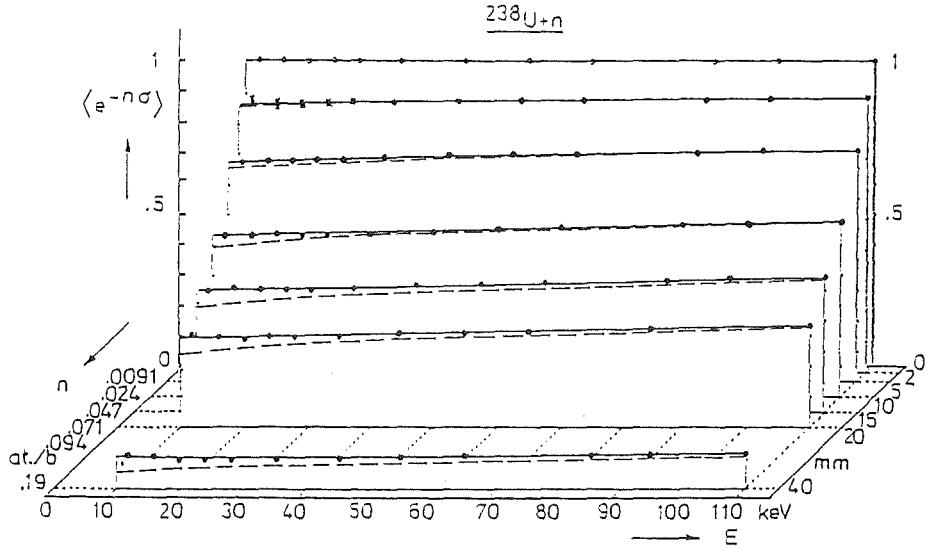

Fig. 13. Thick-sample transmission data of Bokhovko et al. (1988) (point symbols) and curves generated with Monte Carlo techniques from JEF-2 average resonance parameters (solid lines). Also shown are the transmission curves obtained without correction for resonance structure (broken lines). From Fröhner (1991).

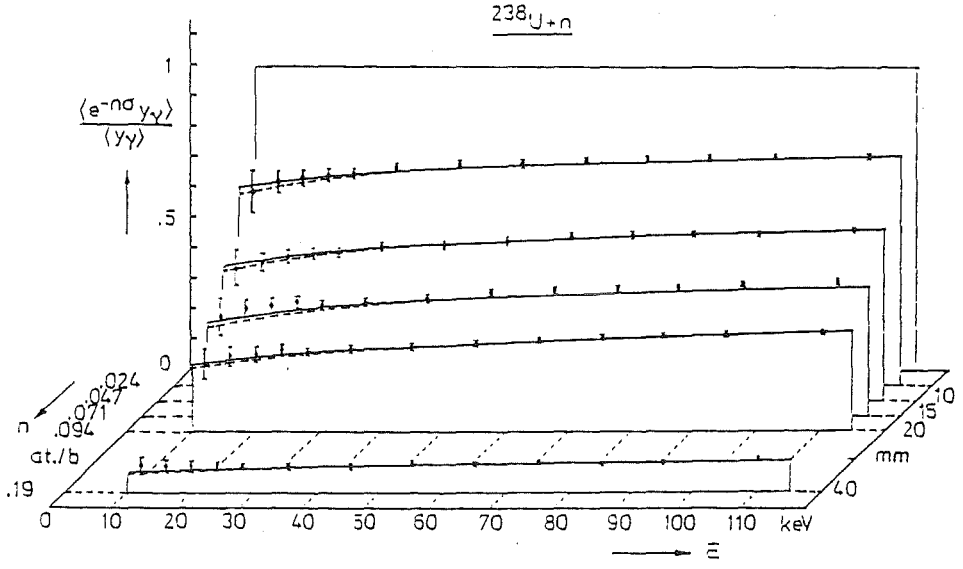

Fig. 14. Self-indication ratios measured by Bokhovko et al. (1988) (point symbols) and curves generated with Monte Carlo techniques from JEF-2 average resonance parameters (solid lines). Also shown are ratios calculated without corrections for resonance self-shielding and multiple scattering (broken lines). From Fröhner (1991).

in opposite directions.) In practice the radiators are not ideally thin, so that the capture cross section σ_γ ought to be replaced by the capture yield y_γ that includes self-shielding and multiple-collision capture. Both effects require Monte Carlo techniques, in addition to ladder sampling one must now also simulate multiple-collision events in the radiator (as explained at Trieste before, see Fröhner 1989a). Fig. 14 shows that the measured data and the Monte Carlo results are in good agreement again, indicating that also the capture cross section structure is adequately represented by the average resonance parameters of the JEF-2 evaluation.

3.4 Group Constants

We saw that for a given average total cross section the average transmission (in some finite energy interval containing many resonances) of a thick sample is larger if the cross section fluctuates than if it is smooth (see Eq. 166). This means that the sample becomes less transparent as the temperature rises, due to the smoothing effect of Doppler broadening. (Thermal expansion of the sample counteracts this effect to some degree.) In a reactor region filled with a mixture of materials a temperature increase means that (n,x) processes, e. g. (n,γ) reactions in ^{238}U, become more probable with increasing temperature because the flux depletion across the resonances becomes weaker as the resonance structure is smoothed out (remember Fig. 1). In order to calculate these complicated effects one simplifies by using group constants, i. e. suitably defined cross section averages. The (n,x) reaction rate for a given nuclide, averaged over the region and over a finite (group) interval ΔE, can be written as

$$\langle\phi\sigma_x\rangle = f_x\langle\sigma_x\rangle\langle\phi\rangle \qquad \text{with} \qquad \langle\ldots\rangle \equiv \int_{\Delta E} \frac{dE}{\Delta E}\ldots \tag{170}$$

The group boundaries are usually taken as equidistant on a logarithmic energy scale, i. e. on a linear lethargy scale, so that there is always the same number of groups per energy decade. The cross section σ_x is to be understood as Doppler broadened. Since $\langle\sigma_x\rangle$ does not depend on temperature (apart from edge effects at group boundaries which become negligible if the group interval contains many resonances) the main temperature dependence for given average flux is contained in the so-called self-shielding or Bondarenko factor f_x.

3.3.1 Bondarenko Factors

The self-shielding factor depends not only on temperature but also on the cross sections of all other nuclides in the mixture, the so-called dilution. The data filed in group constant sets for technological applications are (cf. e. g. Bondarenko et al. 1964)

- cross sections for infinite dilution $\langle\sigma_x\rangle$,
- self-shielding factors $f_x = \dfrac{\langle\phi\sigma_x\rangle}{\langle\phi\rangle\langle\sigma_x\rangle}$,

stored for each nuclide on a grid of temperatures and dilution cross sections σ_d, e. g.

T = 300, 900, 1500, 3100 K ,
σ_d = 0, 1, 10, 100, 1000, 10 000, 100 000, 1 000 000 b .

The self-shielded group cross section

$$\bar\sigma_x \equiv f_x\langle\sigma_x\rangle \tag{171}$$

is defined so that multiplication with the group-averaged flux ϕ gives the correct reaction rate. With the definition of the covariance one can write

$$f_x = 1 + \mathrm{cov}\left(\frac{\phi}{\langle\phi\rangle}, \frac{\sigma_x}{\langle\sigma_x\rangle}\right) . \tag{172}$$

Now the flux is low where the cross section is high, so the two are anticorrelated, the covariance is negative, hence $f_x < 1$. On the other hand f_x must be positive since otherwise the average reaction rate would become negative. It follows (at least in the case of many levels within the group interval) that one has $0 < f_x < 1$. We can be more explicit by invoking the narrow-resonance approximation, valid in the important case that the resonances are narrow as compared to the mean energy loss of scattered neutrons. In this approximation the flux is proportional to the reciprocal macroscopic total cross section, $\phi \propto 1/(\sigma + \sigma_d)$, where $\sigma = \sum_x \sigma_x$ is the total cross section of the nuclide considered. One has then in narrow-resonance approximation

$$f_x = \frac{\langle\sigma_x/(\sigma+\sigma_d)\rangle}{\langle\sigma_x\rangle\,\langle 1/(\sigma+\sigma_d)\rangle} = \frac{\int_0^\infty dn\, e^{-n\sigma_d}\langle e^{-n\sigma}\sigma_x\rangle/\langle\sigma_x\rangle}{\int_0^\infty dn\, e^{-n\sigma_d}\langle e^{-n\sigma}\rangle} , \tag{173}$$

Since σ_d is a constant in the Bondarenko scheme one recognises that $f_x \to 1$ if either $T \to \infty$ (smooth total cross section) or $\sigma_d \to \infty$ (infinite dilution). Therefore $\langle\sigma_x\rangle$ is called the group cross section for infinite dilution (or the unshielded group cross section). In groups containing many resonances it is just the average cross section in the usual sense.

The last expression shows how self-shielding factors are related to self-indication ratios, Eq. 166, and average transmissions, Eq. 168. If those latter quantities can be predicted accurately for sufficiently thick samples the self-shielding factor, too, can be predicted well. With the results shown in Figs. 13 and 14, and because of the positive correlation between numerator and denominator in the last equation, it appears that the self-shielding factors for the unresolved resonance region of ^{238}U can be calculated to 1-2% accuracy from the JEF-2 average resonance parameters.

3.3.2 Analytic and Monte Carlo Methods for Group Constant Generation

The practically important method for group constant generation is the analytic method (Frölich 1965, Hwang 1965). The averages in the last equation are calculated on the basis of level statistics in narrow-resonance approximation. The simplest version includes the following additional approximations:

- Cross sections are written as sums over SLBW terms ("many-level" Breit-Wigner approximation).
- Doppler broadening is described by the symmetric and asymmetric Voigt profiles ψ and χ.
- Interference between resonance and potential scattering (terms with χ) are neglected
- Level-statistical averages are calculated for each level sequence with the other sequences approximately represented by a smooth cross section included in σ_d.

The result can be written in the form

$$\bar{\sigma}_x = f_x\langle\sigma_x\rangle = (\sigma_p + \sigma_d)\Big(1 - \sum_s \frac{\langle\Gamma J\rangle_s}{D_s}\Big)^{-1} \sum_s \frac{\langle\Gamma_x J\rangle_s}{D_s \cos 2\varphi_s} , \tag{174}$$

where σ_p is the potential scattering cross section of the nuclide considered, $\langle \ldots \rangle_s$ denotes an average over all partial widths for the s-th level sequence, the summations are over all sequences, and J is the integral

$$J(\kappa,\beta) \equiv \int_0^\infty dx \, \frac{\psi(x,\beta)}{\psi(x,\beta)+\kappa} \tag{175}$$

introduced by Dresner (1960). It involves the symmetric Voigt profiles (compare Eq. 117 and Appendix)

$$\psi(x,\beta) = \frac{1}{\beta\sqrt{\pi}} \int_{-\infty}^{\infty} \exp\left[-\left(\frac{x-y}{\beta}\right)^2\right] \frac{dy}{1+y^2} \, , \tag{176}$$

where $\beta \equiv 2\Delta/\Gamma$ is the Doppler width in units of the natural half width at half maximum, $\Gamma/2$, and $x \equiv 2(E-E_0)/\Gamma$ is the distance to the resonance peak at E_0 in the same units. Furthermore,

$$\kappa = \frac{\sigma_d + r}{\hat{\sigma}} \, , \tag{177}$$

$$\hat{\sigma} = 4\pi\lambda^2 g \frac{\Gamma_n}{\Gamma} \cos 2\varphi \, , \tag{178}$$

r describing eigenvalue repulsion in approximate form. This is the fastest method available for group constant generation. It is employed in many widely used codes, e. g. ETOX (Schenter et al. 1969), MIGROS (Broeders and Krieg 1977), NJOY (MacFarlane et al. 1982), and GRUCON (Sinitsa 1983).

The slowing-down method uses Monte Carlo sampled resonance ladders so that the calculation of average reaction rates can be reduced to the case of resolved resonances. The TIMS code (Takano et al. 1980) is an example. Monte Carlo sampled resonance ladders are also used in the subgroup/multiband methods pioneered by Nikolaev et al. (1970) and Cullen (1974). One stores, for each of few (e. g. four) subgroups/bands, the weights α_i and the band averages σ_i, σ_{xi} representing in a crude way the cross section distribution within an energy group. They must be found by matching averages obtained from ladder cross sections as follows,

$$\langle \sigma_x \rangle = \sum_i \alpha_i \sigma_{xi} \, , \tag{179}$$

$$\langle \sigma \rangle = \sum_i \alpha_i \sigma_i \, , \tag{180}$$

$$\left\langle \frac{\sigma_x}{\sigma+\sigma_d} \right\rangle = \sum_i \frac{\alpha_i \sigma_{xi}}{\sigma_i+\sigma_d} \, , \tag{181}$$

$$\left\langle \frac{1}{\sigma+\sigma_d} \right\rangle = \sum_i \frac{\alpha_i}{\sigma_i+\sigma_d} \, . \tag{182}$$

The multigroup/multiband method is essentially a coarse but efficient variant of the probability table method (Levitt 1972) where one generates from sampled resonance ladders the whole multivariate probability density

$$p(\sigma,\sigma_n,\sigma_\gamma,\ldots) = p(\sigma)p(\sigma_n|\sigma)p(\sigma_\gamma|\sigma,\sigma_n)\ldots \, . \tag{183}$$

The distribution of the total cross section, $p(\sigma)$, is stored together with the conditional probabilities $p(\sigma_n|\sigma)$, $p(\sigma_\gamma|\sigma,\sigma_n)$ etc. in suitably discretised form, so that macroscopic (isotope-weighted, Doppler broadened) cross sections rather than resonance parameters may be sampled directly.

3.3.3 Problems with Self-Shielding

There is a number of problems with existing self-shielding methods. Some of the more pressing ones are as follows.

- How good is the level-statistical analytic method compared to Monte Carlo ladder methods?
- What are good techniques for the partially resolved region (roughly 6 - 60 keV for ^{238}U, 0.8 - 3 MeV for ^{56}Fe)? One could obviously improve over a purely statistical treatment with information about at least the strongest resonances.
- How serious are overlap effects, due to coincidence of strong resonances belonging to different isotopes? How should they be handled?
- What can be done to encourage experimenters to provide good data against which calculated self-shielding factors can be tested? There is a conspicuous lack of thick-sample transmission and self-indication data, similar to those for ^{238}U in Figs. 13 and 14. The unresolved region for ^{56}Fe, important for shielding, is an example.

This is just an indication of what the present problems are in the unresolved resonance range. There are many more concerning the best way to implement the multigroup/multiband concept or Monte Carlo techniques, the correct handling of mixtures, of heterogeneities, of angular distributions, of double-differential ("DDX") data, etc. The requests from nuclear technology are not only for average cross sections with accuracies of 1 - 3 % for key reactions such as ^{235}U(n,f), ^{238}U(n,γ), ^{239}Pu(n,f), but also for self-shielding factors with accuracies of about 1 %. This is a challenge not only for measurers and analysts of data but also for code developpers and applied theorists. We are close to the goal as far as average cross sections are concerned but level-statistical data and computational techniques for self-shielding are still far from satisfactory. As a consequence Doppler coefficients (the reactivity response to rapid temperature changes) especially of fast fission reactors could be predicted so far only with 10-20% uncertainty.

4. Concluding remarks

We reviewed those aspects of neutron resonance theory that are most important for safety-related nuclear research. The relationship between R-matrix theory, Hauser-Feshbach theory, the statistical model of resonance reactions and the optical model was explained. Doppler broadening was treated in some detail for the practically important resonance formalisms and for tabulated cross sections. The exposition was by necessity brief but it is hoped that enough material and references have been presented that interested students have an adequate starting base for further studies and professional work. Especially in the unresolved resonance region there is considerable need for methods development and creative programming, in both the fission and the fusion reactor field. Those who are particularly interested in analysis and evaluation of resonance data will find additional material in the 1988 ICTP proceedings (Fröhner 1989a).

ACKNOWLEDGMENTS. It is a pleasure to thank the organisers of the lecture course and the ICTP Trieste who made it possible to present this work, and Dr. E. Kiefhaber for discussions. Support by the Project Nuclear Safety Research at KfK is acknowledged.

Appendix: Mathematical Properties of the Voigt Profiles ψ and χ

The shapes of Doppler broadened isolated resonances can be described by the symmetric and asymmetric Voigt profiles $\psi(x,\beta)$ and $\chi(x,\beta)$. The arguments

$$x \equiv \frac{E - E_0}{\Gamma/2}, \qquad (A1) \qquad \beta \equiv \frac{\Delta}{\Gamma/2} \qquad (A2)$$

depend on the resonance energy E_0, the total width Γ, the Doppler width Δ (see Eq. 110), and the bombarding energy E (all in the laboratory system).

Definition:

$$\psi(x,\beta) = \frac{1}{\beta\sqrt{\pi}} \int_{-\infty}^{\infty} e^{-(x - x')^2/\beta^2} \frac{dx'}{1 + x'^2} = \psi(-x,\beta) \qquad (A3)$$

$$\chi(x,\beta) = \frac{1}{\beta\sqrt{\pi}} \int_{-\infty}^{\infty} e^{-(x - x')^2/\beta^2} \frac{x'dx'}{1 + x'^2} = -\chi(-x,\beta) \qquad (A4)$$

Special arguments:

at resonance energy, $E = E_0$

$$\psi(0,\beta) = \frac{\sqrt{\pi}}{\beta} e^{1/\beta^2} \operatorname{erfc} \frac{1}{\beta} \qquad (A5) \qquad \chi(0,\beta) = 0 \qquad (A6)$$

for zero temperature, $T = 0$

$$\psi(x,0) = \frac{1}{1 + x^2} \qquad (A7) \qquad \chi(x,0) = \frac{x}{1 + x^2} \qquad (A8)$$

Convergent series:

$$\psi(x,\beta) = \frac{1}{\beta} e^{(1 - x^2)/\beta^2} \sum_{n=0}^{\infty} \frac{1}{n!} \left(\frac{x}{\beta^2}\right)^{2n} \Gamma\left(-n + \frac{1}{2}, \frac{1}{\beta^2}\right) \qquad (A9)$$

$$\chi(x,\beta) = \frac{1}{\beta} e^{(1 - x^2)/\beta^2} \sum_{n=0}^{\infty} \frac{1}{n!} \left(\frac{x}{\beta^2}\right)^{2n+1} \Gamma\left(-n - \frac{1}{2}, \frac{1}{\beta^2}\right) \qquad (A10)$$

where $\Gamma(a,t)$ is the incomplete gamma function, with

$$\Gamma(a + 1, t) = a\Gamma(a,t) + e^t t^a = \int_t^{\infty} dt' e^{-t'} t'^a \qquad (A11)$$

$$\Gamma\left(\frac{1}{2}, t\right) = \sqrt{\pi} \operatorname{erfc} \sqrt{t} \qquad (A12)$$

Asymptotic series for low temperatures (small β):

$$\psi(x,\beta) = \sum_{n=0}^{\infty} \frac{(2n + 1)!!}{2n + 1} \left(-\frac{\beta^2}{2}\right)^n \left(\frac{1}{1 + x^2}\right)^{n+1/2} \cos[(2n + 1) \arctan x] \qquad (A13)$$

$$\chi(x,\beta) = \sum_{n=0}^{\infty} \frac{(2n+1)!!}{2n+1}\Big(-\frac{\beta^2}{2}\Big)^n \Big(\frac{1}{1+x^2}\Big)^{n+1/2} \sin[(2n+1)\arctan x] \qquad (A14)$$

whence

$$\psi(x,\beta) + i\chi(x,\beta) = \sum_{n=0}^{\infty} \frac{(2n+1)!!}{2n+1}\Big(-\frac{\beta^2}{2}\Big)^n \Big(\frac{1}{1+x^2} + \frac{ix}{1+x^2}\Big)^{2n+1} \qquad (A15)$$

Relationship with complex probability integral:

$$\psi(x,\beta) + i\chi(x,\beta) = \frac{\sqrt{\pi}}{\beta} W\Big(\frac{x+i}{\beta}\Big), \qquad (A16)$$

where

$$W(z) = \frac{1}{\pi i}\int_{-\infty}^{\infty} \frac{e^{-t^2}}{t-z}dt = e^{z^2}\Big(1 + \frac{2i}{\sqrt{\pi}}\int_0^z e^{-t^2}dt\Big) \qquad (A17)$$

Derivatives:

$$\frac{\partial\psi}{\partial x} = \frac{2}{\beta^2}(\chi - x\psi) \qquad (A18) \qquad \frac{\partial\chi}{\partial x} = \frac{2}{\beta^2}(1 - \psi - x\chi) \qquad (A19)$$

Integrals:

$$\int_{-\infty}^{\infty} \psi(x,\beta)dx = \pi \qquad (A20) \qquad \int_{-\infty}^{\infty} \chi(x,\beta)dx = 0 \qquad (A21)$$

REFERENCES

F.T. Adler and D.B. Adler, in *Nucl. Data for Reactors*, IAEA Vienna (1970) p. 777

H.A. Bethe, *Rev. Mod. Phys.* **9** (1937) 69

M.R. Bhat and G.E. Lee-Whiting, *Nucl. Instr. Meth.* **47** (1967) 277

L.C. Biedenharn, Report ORNL-1501 (1953)

J.M. Blatt and L.C. Biedenharn, *Rev. Mod. Phys.* **24** (1952) 258

C. Bloch, *Nucl. Phys.* **A112** (1968) 257, 253

Å. Bohr, *Conf. on Peaceful Uses of Atomic Energy*, Geneva (1955) vol. 2, p. 151

M.V. Bokhovko, V.N. Kononov, G.N. Manturov, E.D. Poletaev, V.V. Sinitsa, A.A. Voevodskij, *Yad. Konst.* 3 (1988) 11; Engl. transl.: IAEA report INDC(CCP)-322 (1990) p. 5

I.I. Bondarenko et al., *Group Constants for Nuclear Reactor Calculations*, Consultant Bureau Enterprises Inc., New York (1964)

M. Born, *Optik*, Springer, Berlin (1933)

T.A. Brody, J. Flores, J.B. French, P.A. Mello, A. Pandey and S.S. Wong, *Rev. Mod. Phys.* **53** (1981) 385

I. Broeders and B. Krieg, Karlsruhe report KfK 2388 (1977)

C.E. Cullen and C.R. Weisbin, *Nucl. Sci. Eng.* **60** (1976) 199

C.E. Cullen, *Nucl. Sci. Eng.* **55** (1974) 387

G. de Saussure and R.B. Perez, Oak Ridge report ORNL-TM-2599 (1969)

A. de-Shalit and I. Talmi, *Nuclear Shell Theory*, Acad. Press, New York – London (1963) ch. 15 and Appendix

L. Dresner, *Proc. Int. Conf. on Neutron Reactions with the Nucleus* , Columbia U. 1957, Report CU-157 (1957) p. 71

L. Dresner, *Resonance Absorption in Nuclear Reactors*, Pergamon, Oxford (1960)

C.A. Engelbrecht and H.A. Weidenmüller, *Phys. Rev.* C8 (1973) 859; N. Nishioka and H.A. Weidenmüller, *Phys. Letters* **157B** (1985) 101

U. Fano and G. Racah, *Irreducible Tensor Sets*, Acad. Press, New York (1959)

F.H. Fröhner, *Conf. on Neutron Phys. and Nucl. Data*, Harwell (1978) p. 306

F.H. Fröhner, *Applied Neutron Resonance Theory*, Karlsruhe Report KfK-2669 (1978); reprinted in *Nuclear Theory for Applications*, Report IAEA-SMR-43, ICTP. Trieste (1980) p. 59

F.H. Fröhner, B. Goel, U. Fischer, *Proc. Meet. on Fast-Neutron Capture Cross Sections*, Argonne, ANL-83-4 (1982) p. 116

F.H. Fröhner, *Proc Int. Conf. Nucl. Data for Basic and Appl. Sci., Santa Fe 1985*, New York etc. (1986) p. 1541; reprinted in *Rad. Effects* **96** (1986) 199

F.H. Fröhner, *Nucl. Sci. Eng.* **103** (1989) 119

F.H. Fröhner, *Applied Theory of Resolved and Unresolved Resonances*, in *Applied Nuclear Theory and Nuclear Model Calculations for Nuclear Technology Applications*, M.K. Mehta and J.J. Schmidt (eds.), World Scientific, Singapore etc. (1989a) p. 170

F.H. Fröhner, in *Nuclear Physics, Neutron Physics and Nuclear Energy*, W. Andrejtscheff and D. Elenkov (eds.), World Scientific, Singapore (1990) p. 333; separately available as Karlsruhe report KfK 4655 (1990)

F.H. Fröhner, Karlsruhe report KfK 4911 (1991); *Nucl. Sci. Eng.* **111** (1992) 404

F.H. Fröhner, in *Maximum Entropy and Bayesian Methods*, W.T. Grandy Jr. and L.H. Schick (eds.), Kluwer, Dordrecht (1991a) p. 93

R. Frölich, Karlsruhe report KfK 367 (1965)

M. Gaudin, *Nucl. Phys.* **25** (1961) 447; reprinted in Porter (1965)

A. Gilbert and A.G.W. Cameron, *Can. J. Phys.* **43** (1965) 1446

H. Gruppelaar and G. Reffo, *Nucl. Sci. Eng.* **62** (1977) 756

H.M. Hofmann, J. Richert, J.W. Tepel, H.A. Weidenmüller, *Ann. Phys.* **90** (1975) 403

L.K. Hua, *Harmonic Analysis of Functions of Several Complex Variables in the Classical Domains*, Am. Math. Soc., Providence, R.I. (1963)

H.H. Hummel and D. Okrent, *Reactivity Coefficients in Large Fast Power Reactors*, Monogr. Ser. Nucl. Sci. Technol., Am. Nucl. Soc., Hindsdale, Ill. (1970)

R.N. Hwang, *Nucl. Sci. Eng.* **21** (1965) 523; **52** (1973) 157

N. Janeva, N. Koyumdjieva, A. Lukyanov, S. Toshkov, *Proc. Int. Conf. Nucl. Data for Basic and Appl. Sci., Santa Fe 1985*, New York etc. (1986) p. 1615; N. Koyumdjieva, N. Savova, N. Janeva, A.A. Lukyanov, *Bulg. J. Phys.* **16** (1989) 1

E.T. Jaynes, *Papers on Probability, Statistics and Statistical Physics*, R.D. Rosenkrantz (ed.), Reidel, Dordrecht (1983)

P.L. Kapur and R.E. Peierls, *Proc. Roy. Soc. (London)* **A166** (1938) 277

G.A. Korn and T.M. Korn, *Math. Handbook for Scientists and Engineers*, McGraw - Hill, New York etc. (1968)

A.M. Lane and R.G. Thomas, *Rev. Mod. Phys.* **30** (1958) 257

W.E. Lamb, *Phys. Rev.* **55** (1939) 750

A.M. Lane and J.E. Lynn, *Proc. Phys. Soc.* **A70** (1957) 557
L.B. Levitt, *Nucl. Sci. Eng.* **49** (1972) 450
J.E. Lynn, *The Theory of Neutron Resonance Reactions*, Clarendon Press, Oxford (1968)
R.E. MacFarlane, D.W. Muir, R.M. Boicourt, Los Alamos report LA-9303-MS, vols. I and II (1982); R.E. MacFarlane and D.W. Muir, vol. III (1987); D.W. Muir and R.E. MacFarlane, vol. IV (1985)
M.L. Mehta, *Nucl. Phys.* **18** (1960) 395; reprinted in Porter (1965)
P.A. Mello, *Phys. Lett.* **B82** (1979) 103; cf. also P.A. Mello and T.H. Seligman, *Nucl. Phys.* **A344** (1980) 489
P.A. Mello, P. Pereyra, T.H. Seligman, *Ann. Phys.* **161** (1985) 254
P.A. Moldauer, *Phys. Rev.* **C11** (1975) 426; **C12** (1975) 744
P.A. Moldauer, *Nucl. Phys.* **A344** (1980) 185
S.F. Mughabghab, M. Divadeenam, N.E. Holden, *Neutron Cross Sections, Neutron Resonance Parameters and Thermal Cross Sections*, Vol. A: Z = 1 - 60, Acad. Press, New York etc. (1981)
S.F. Mughabghab, *Neutron Cross Sections, Neutron Resonance Parameters and Thermal Cross Sections*, Vol. B: Z = 61 - 100, Acad. Press, New York etc. (1984)
A. Müller and H.L. Harney, *Phys. Rev.* **C35** (1987) 1231
M.N. Nikolaev et al., *At. Energiya* **29** (1970) 11
C.M. Perey, F.G. Perey, J.A. Harvey, N.W. Hill, N.M. Larson, ^{56}Fe *Resonance Parameters for Neutron Energies up to 850 keV*, Oak Ridge National Laboratory, ORNL/TM-11742 (1990)
C.E. Porter and R.G. Thomas, *Phys. Rev.* **104** (1956) 483; reprinted in Porter (1965)
C.E. Porter (ed.) *Statistical Theory of Spectra: Fluctuations*, Acad. Press, New York - London (1965)
C.E. Porter and N. Rosenzweig, *Suomal. Tiedeakad. Toimit. (Ann. Acad. Sci. Fenn.)* **AVI** 44 (1960); reprinted in Porter (1965)
C.W. Reich and M.S. Moore, *Phys. Rev.* **111** (1958) 929
P.F. Rose and C.L. Dunford (eds.) , Report ENDF-102, NNDC Brookhaven (1990)
G.R. Satchler, *Phys. Letters* **7** (1963) 55
R.E. Schenter, J.L. Baker, R.B. Kidman, Batelle North West report BNWL-1002 (1969)
V.V. Sinitsa, *Yad. Konst.* **5(54)** (1983); Engl. transl. IAEA report INDC(CCP)-225/G (1985)
A.W. Solbrig, *Nucl. Sci. Eng.* **10** (1961) 167
H. Takano, Y. Ishiguro, Y. Matsui, report JAERI-1267 (1980)
R.G. Thomas, *Phys. Rev.* **97** (1955) 224
A.M. Turing, *Proc. London Math. Soc.*, Ser. 2, **48** (1943) 180
J.M. Verbaarschot, H.A. Weidenmüller, M.R. Zirnbauer, *Phys. Reports* **129** (1985) 367
J.M. Verbaarschot, *Ann. Phys.* **168** (1986) 368
E. Voigt, *Sitz.-Ber. Bayer. Akad. Wiss.* (1912) p. 603
E.P. Wigner and L. Eisenbud, *Phys. Rev.***72** (1947) 29; E.P. Wigner, *J. Am. Phys. Soc.* **17** (1947) 99
E.P. Wigner, *Can. Math. Congr. Proc.*, Toronto (1957) p. 174; *Ann. Math.* **67** (1958) 325; both reprinted in Porter (1965)
E.P. Wigner, *Conf. on Neutron Phys. by Time-of-Flight*, Gatlinburg 1956, Oak Ridge report ORNL-2309 (1957) p. 59; reprinted in Porter (1965)